Heft R597 (2021)

FVV-Informationstagung Motoren | Frühjahrstagung 2021 – Frankfurt (Digitalkonferenz)

Initiale Vorentflammung

FVV Nr. 1328 | Abschlussbericht (AB)

1 | Institut für Kolbenmaschinen (IFKM), Karlsruher Institut für Technologie
Prof. Dr. sc. techn. Thomas Koch

2 | Institut für Technische Thermodynamik (ITT), Karlsruher Institut für Technologie
Prof. Dr. rer. nat. habil. Ulrich Maas

3 | Institut für Fahrzeugantriebe und Automobiltechnik (IFA), Technische Universität Wien
Univ.-Prof. Dipl.-Ing. Dr. techn. Bernhard Geringer

4 | Institut für Verbrennungskraftmaschinen und Thermodynamik (IVT), Technische Universität Graz
Univ.-Prof. Dipl.-Ing. Dr. techn. Helmut Eichlseder

Thema:	Identifikation des Mechanismus zur initialen Vorentflammung mittels Kombination von experimentellen Untersuchungen und Simulation der Tropfenzündung
Laufzeit:	01.05.2018 – 31.12.2020
Fördergeber:	Bundesministerium für Wirtschaft und Energie / Arbeitsgemeinschaft industrieller Forschungsvereinigungen e. V. / Collective Research Networking (BMWi/AiF-CORNET) Forschungsvereinigung Verbrennungskraftmaschinen e. V. (FVV) Bundesministerium für Verkehr, Innovation und Technologie (BMVIT) Österreichische Forschungsförderungsgesellschaft (FFG)
Fördernummer(n):	IGF 224 EN, FVV 601328, FFG 865261
Vorsitzende(r) projektbegleitender Ausschuss:	Dipl.-Ing. Albert Breuer (Ford-Werke GmbH)
Bearbeiter und Verfasser:	Dr. Chien Chia Liu (ITT) Dr.-Ing. Robert Schießl (ITT) Thorsten Schweizer, M.Sc. (IFKM) Dr.-Ing. Heiko Kubach (IFKM) Dipl.-Ing. Markus Eder (IVT) Dr. techn. Peter Grabner (IVT) Dipl.-Ing. Norbert Zöbinger (IFA) Assoc. Prof. Dipl.-Ing. Dr. techn. Thomas Lauer (IFA)
Vortragende(r):	Prof. Dr. sc. techn. Thomas Koch (IFKM)

Danksagung

Dieser Bericht ist das wissenschaftliche Ergebnis einer Forschungsaufgabe, die von der Forschungsvereinigung Verbrennungskraftmaschinen (FVV) e. V. gestellt und am Institut für Kolbenmaschinen (IFKM) des Karlsruher Instituts für Technologie unter der Leitung von Prof. Dr. sc. techn. Thomas Koch und am Institut für Technische Thermodynamik (ITT) des Karlsruher Instituts für Technologie unter der Leitung von Prof. Dr. rer. nat. habil. Ulrich Maas und dem Institut für Fahrzeugantriebe und Automobiltechnik (IFA) unter der Leitung von Univ.-Prof. Dipl.-Ing. Dr. techn. Bernhard Geringer an der Technischen Universität Wien sowie dem Institut für Verbrennungskraftmaschinen und Thermodynamik (IVT) unter der Leitung von Univ.-Prof. Dipl.-Ing. Dr. techn. Helmut Eichlseder an der Technischen Universität Graz bearbeitet wurde.

Die FVV und der AC styria Mobilitätscluster dankt den Professoren Maas, Koch, Eichlseder und Geringer und ihren wissenschaftlichen Mitarbeitern - Dr. Chien Chia Liu, Dr.-Ing. Robert Schießl (alle ITT), M.Sc. Thorsten Schweizer, Dr.-Ing. Heiko Kubach (alle IFKM), Dipl.-Ing. Markus Eder, Dr. techn. Peter Grabner (alle IVT), Dipl.-Ing. Norbert Zöbinger und Assoc. Prof. Dipl.-Ing. Dr. techn. Thomas Lauer (alle IFA) - für die Durchführung des Vorhabens sowie der Arbeitsgemeinschaft industrieller Forschungsvereinigungen (AiF) e. V. und der FFG (Österreichische Forschungsförderungsgesellschaft) für die finanzielle Förderung im Rahmen des internationalen Förderprogramms CORNET (Collective Research Networking). Das Projekt wurde von einer Expertengruppe unter der Leitung von Dipl.-Ing. Albert Breuer (Ford-Werke GmbH) durchgeführt. Diesem projektbegleitenden Ausschuss gebührt unser Dank für die große Unterstützung. Die vorgestellten Rechenergebnisse der Technische Universität Wien wurden mit dem Vienna Scientific Cluster (VSC) erzielt.

Insbesondere danken wir der Ford-Werke GmbH für die Bereitstellung der Versuchsträger, KS Kolbenschmidt GmbH für die Bereitstellung der Kolben, Fuchs Schmierstoffe GmbH für die Bereitstellung der Motorenöle, Coryton Advanced Fuels Ltd. für die Bereitstellung des LSPI Kraftstoffes, OMV für die Bereitstellung des Super Ottokraftstoffes, IoLiTec für die Bereitstellung der ionischen Flüssigkeiten, NAGEL Maschinen- und Werkzeugfabrik GmbH für die Zylinderhonungen und Siemens für die Bereitstellung der CFD Lizenzen.

Das Forschungsvorhaben wurde im Rahmen des Programms zur Förderung der industriellen Gemeinschaftsforschung (IGF/CORNET-Nr. 224 EN) vom Bundesministerium für Wirtschaft und Energie (BMWi) über die Arbeitsgemeinschaft industrieller Forschungsvereinigungen (AiF) e. V. aufgrund eines Beschlusses des Deutschen Bundestages gefördert. Die Arbeit der Technischen Universität Wien wurde vom Bundesministerium für Verkehr, Innovation und Technologie (BMVIT) über die Österreichische Forschungsförderungsgesellschaft (FFG, Bewilligungsnummer 865261) gefördert.

Gefördert durch:
Bundesministerium für Wirtschaft und Energie
aufgrund eines Beschlusses des Deutschen Bundestages
AiF Forschungsnetzwerk Mittelstand
IGF Industrielle Gemeinschaftsforschung
FVV Forschungsvereinigung Verbrennungskraftmaschinen

Kurzfassung

Im Rahmen des Forschungsvorhabens wurde der grundlegende Entstehungsmechanismus der initialen Vorentflammung bei hochaufgeladenen Ottomotoren und niedrigen Motordrehzahlen untersucht. Um einen tieferen Einblick in dieses stochastisch auftretende, irreguläre Verbrennungsphänomen zu erhalten, wurden Untersuchungen am Motorenprüfstand sowie numerische Studien durchgeführt. Neben den Untersuchungen zur thermodynamischen Charakterisierung der LSPI-Frequenz (LSPI: Low-speed pre-ignition) unter verschiedenen motorischen Randbedingungen, wurden die Vorgänge im Brennraum mithilfe optischer Zugänge aufgezeichnet. Um den Einfluss des flüssigen Kraftstoffs auf den Entstehungsmechanismus zu untersuchen wurde der Motor zusätzlich auf den Betrieb mit CNG adaptiert. Darüber hinaus wurde die Möglichkeit einer Öltropfenzündung durch die Eindosierung von Schmierstoff in das Saugrohr experimentell untersucht.

Um das LSPI-Phänomen numerisch untersuchen zu können, wurden die thermodynamischen Bedingungen im Brennraum mithilfe eines 3D-CFD Motormodells ermittelt. Weiters wurde ein 11-Komponenten Ersatzkraftstoffmodell entwickelt, um die Benetzung der Brennraumwände durch das Kraftstoffspray möglichst genau abbilden zu können. Auf Basis dieser Randbedingungen wurden anschließend numerische Studien zur Öltropfen- und Partikel-induzierten Zündung durchgeführt.

Die durchgeführten Untersuchungen zeigten, dass alle initialen Vorentflammungen durch lichtemittierende Ablagerungen oder fliegende Objekte getriggert wurden. Der Bereich der Ablagerungsbildung und in Folge auch der beobachtbaren Ablösungen konnten mit Bereichen intensiver Kraftstofffilmbildung korreliert werden. Weder Experimente noch numerische Studien konnten eine Öltropfen-induzierte Zündung nachweisen. Im Fall von inerten Partikeln konnte simulativ gezeigt werden, dass diese die notwendige minimale Oberflächentemperatur innerhalb von zwei Zyklen nicht erreichen konnten.

Basierend auf den erzielten Ergebnissen konnte ein grundlegender Entstehungsmechanismus synthetisiert werden, der nahelegt, dass im Brennraum befindliche Ansammlungen von Öl und Kraftstoff durch mehrfache Verbrennungsvorgänge so aufbereitet werden, dass hochreaktive Ablagerungen entstehen können. Diese können so aufgeheizt werden, dass sie direkt an der Wand oder in der Gasphase zu einer vorzeitigen Gemischentflammung führen können.

Issue R597 (2021)

FVV Information Sessions Engine | Spring 2021 – Frankfurt (Digital Conference)

Initial Pre-ignition

FVV no. 1328 | Final report (AB)

1 | Institute of Internal Combustion Engines (IFKM), Karlsruhe Institute of Technology
Prof. Dr. sc. techn. Thomas Koch

2 | Institute of Technical Thermodynamics (ITT), Karlsruhe Institute of Technology
Prof. Dr. rer. nat. habil. Ulrich Maas

3 | Institute of Powertrains and Automotive Technology (IFA), Technische Universität Wien
Univ.-Prof. Dipl.-Ing. Dr. techn. Bernhard Geringer

4 | Institute of Internal Combustion Engines and Thermodynamic (IVT),
Graz University of Technology
Univ.-Prof. Dipl.-Ing. Dr. techn. Helmut Eichlseder

Full title:	Identification of the mechanism for initial pre-ignition by a combination of experimental investigations and simulation of drop ignition
Duration:	01.05.2018 – 31.12.2020
Funding organisation(s):	Federal Ministry for Economic Affairs and Energy / German Federation of Industrial Research Associations eV / Collective Research Networking (BMWi/AiF-CORNET) Research Association for Combustion Engines eV (FVV) Federal Ministry of Transport, Innovation and Technology (BMVIT) Austria Research Promotion Agency (FFG)
Funding number(s):	IGF 224 EN, FVV 601328, FFG 865261
Project user committee chair:	Dipl.-Ing. Albert Breuer (Ford)
Research associate(s) / author(s):	Dr. Chien Chia Liu (ITT) Dr.-Ing. Robert Schießl (ITT) Thorsten Schweizer, M.Sc. (IFKM) Dr.-Ing. Heiko Kubach (IFKM) Dipl.-Ing. Markus Eder (IVT) Dr. techn. Peter Grabner (IVT) Dipl.-Ing.Norbert Zöbinger (IFA) Assoc. Prof. Dipl.-Ing. Dr. techn. Thomas Lauer (IFA)
Lecturer(s):	Prof. Dr. sc. techn. Thomas Koch (IFKM)

Acknowledgement

This report is the scientific result of a research project undertaken by the FVV (The Research Association for Combustion Engines eV) and performed by Institute of Internal Combustion Engines (IFKM) at Karlsruhe Institute of Technology under the direction of Prof. Dr. sc. techn. Thomas Koch and by Institute of Technical Thermodynamics (ITT) at Karlsruhe Institute of Technology under the direction of Prof. Dr. rer. nat. habil. Ulrich Maas and by Institute of Powertrains and Automotive Technology (IFA) under the direction of Univ.-Prof. Dipl.-Ing. Dr. techn. Bernhard Geringer at Technische Universität Wien and by Institute of Internal Combustion Engines and Thermodynamic (IVT) under the direction of Univ.-Prof. Dipl.-Ing. Dr. techn. Helmut Eichlseder at Graz University of Technology.

The FVV and the AC-Styria mobility cluster would like to thank Professors Maas, Koch, Eichlseder and Geringer and their scientific assistants – Dr. Chien Chia Liu, Dr.-Ing. Robert Schießl (all ITT), M.Sc. Thorsten Schweizer, Dr.-Ing. Heiko Kubach (all IFKM), Dipl.-Ing. Markus Eder, Dr. techn. Peter Grabner (all IVT), Dipl.-Ing. Norbert Zöbinger and Assoc. Prof. Dipl.-Ing Dr. techn. Thomas Lauer (all IFA) – for the implementation of the project. Special thanks are due to the AiF (German Federation of Industrial Research Associations eV) and FFG (Austria Research Promotion Agency) for funding the project within the framework of the collective research networking (CORNET) programme. The project was conducted by an expert group led by Dipl.-Ing. Albert Breuer (Ford-Werke GmbH). We gratefully acknowledge the support received from the chairman and all members of the project user committee. The presented computational results of Technische Universität Wien have been achieved using the Vienna Scientific Cluster (VSC).

In addition, we would like to thank Ford-Werke GmbH for the provision of test engines, KS Kolbenschmidt GmbH for the provision of pistons, Fuchs Schmierstoffe GmbH for the provision of engine oil, Coryton Advanced Fuels Ltd. for the provision of LSPI fuel, OMV for the provision of RON95 fuel, IoLiTec for the provision of ionic liquids, NAGEL Maschinen- und Werkzeugfabrik GmbH for the cylinder honing and Siemens for the provision of CFD simulation licenses.

The research was carried out in the framework of the industrial collective programme (IGF/CORNET no. 224 EN). It was supported by the Federal Ministry for Economic Affairs and Energy (BMWi) through the AiF (German Federation of Industrial Research Associations eV) based on a decision taken by the German Bundestag. The work of the Technische Universität Wien was funded by the Federal Ministry of Transport, Innovation and Technology (BMVIT) through the Austria Research Promotion Agency (FFG, grant number 865261).

Abstract

In the framework of this research project, the fundamental mechanism of the initial pre-ignition in highly charged gasoline engines was investigated at low engine speeds. In order to get insight to the characteristics of this stochastically occurring, irregular phenomenon, testbed experiments in combination with numerical simulations were conducted. Besides the thermodynamic characterization of the LSPI frequency (LSPI: Low-speed pre-ignition) under varying engine conditions, processes inside the combustion chamber are optically recorded. Additionally, the influence of the liquid fuel on the pre-ignition mechanism is investigated by modifying the engine configuration to CNG operation. Furthermore, the possibility of oil droplet induced ignitions is investigated by supplying lubricating oil to the engine manifold.

In order to investigate the LSPI phenomenon numerically, the thermodynamic conditions inside the combustions chamber are calculated using a 3D-CFD engine model. On top of this, a detailed 11-component fuel surrogate approach was used to investigate the wetting of the combustion chamber walls by the fuel spray. Based upon this data, comprehensive numerical studies on oil droplet induced ignitions and hot particle induced ignitions are carried out.

The performed investigations showed that all initial pre-ignitions are induced by light-emitting surface deposits or flying objects. The areas of deposit formation and detachment events could be correlated with regions of intensive fuel wall wetting. Further on, there was no experimental or simulative evidence of oil droplet induced pre-ignitions. In the case of inert particles, numerical studies showed that they were not able to surpass the necessary minimum surface temperature to initiate a pre-ignition within two consecutive cycles.

Based on the results obtained, a fundamental formation mechanism could be synthesized, which suggests that accumulations of oil and fuel in the combustion chamber are processed through multiple combustion processes in such a way that highly reactive deposits can arise. These can be heated up in such a way that they can trigger premature ignition of the mixture directly at the wall or in the gas phase.

1 Introduction

With a view to future emission legislation regarding the carbon dioxide (CO2) emissions for internal combustion engines, it is important to improve the efficiency of gasoline internal combustion engines. The downsizing high-load concept, in combination with down speeding, represents a possibility to reduce fuel consumption and decrease CO2-emissions. Increasing the brake mean effective pressure (BMEP) or increasing the geometric compression ratios are measures to increase the efficiency of a gasoline engine. The limitation within these measures is combustion anomalies at full load. Heavy knocking or pre-ignitions can end up in an engine fault [1]. To exploit the full potential regarding efficiency, it is important to know more about the process and occurrences of low-speed-pre-ignitions. In previous publications was already suggested that particles from deposits or oil droplets flying around in the combustion chamber may trigger irregular combustion phenomena [2–4].

The project was performed as cooperation between four university institutes. The main goal of the investigations was to define a holistic explanation about low-speed-pre-ignitions (LSPI) with a combination of experimental tests on the testbed and simulative investigation. The experimental investigations were divided between the two institutes, the IFKM in Karlsruhe and the IVT in Graz. The simulative investigations included 1D process- and 3D CFD-simulations by the IFA as well as physical and chemical reaction simulations about the droplet gas interaction by the ITT. The main work packages, as well as the close cooperation in data- and knowledge- exchange between the project partners, are shown in Figure 1-1.

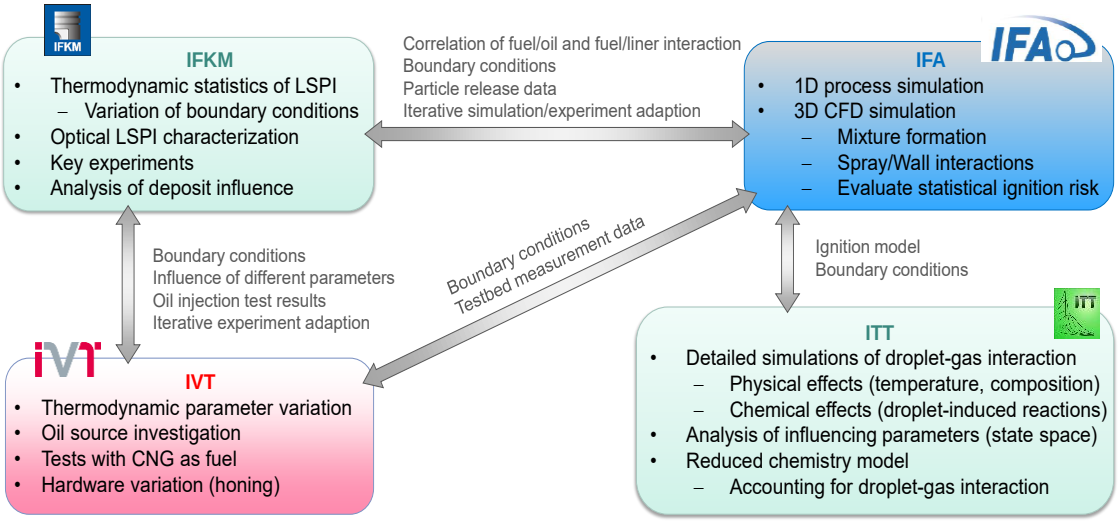

Figure 1-1: Workflow and main work packages of each institute.

2 Testbed methodology

2.1 Test Engine

To carry out the experimental investigations on the testbed, a turbocharged gasoline engine with modifications to resist high in-cylinder pressures, has been used. The engine was a three-cylinder gasoline engine with a displacement of 999 cm³ and a compression ratio of 10.5:1. In addition, the engine was equipped with a wastegate turbocharger and a 200 bar injection system with a central injection position. A detailed engine description is shown in Table 2-1. Due to the earlier combustion during the compression stroke, caused by low-speed-pre-ignitions, the cylinder pressure during such combustion anomalies

can rise to the upper detection limit of the pressure sensor of about 300 bar. In order to withstand combustion cycles with such a high damage potential, the engine was equipped with reinforced connecting rods and reinforced pistons. The pistons were designed for pre-ignition resistance, which in turn led to an increased piston land width. With these modifications, the engine can resist a calculated average cylinder pressure of 140 bar and a calculated maximum cylinder pressure of about 185 bar. The remaining parts of the test engine were serial parts.

Table 2-1:Test engine data.

Ford Fox 1.0 ECO-Boost	
Bore	71.9 mm
Stroke	82 mm
Cylinder number	3
Total displacement	0.999 cm^3
Compression ratio	10.5 : 1
max Torque @1500-4000rpm	170 Nm
max Power @6000 rpm	92 kW
max engine speed	6800 rpm

The test engine in Graz was prepared for in-cylinder-pressure sensing on all three cylinders. The test engine in Karlsruhe was additionally equipped with an optical access at cylinder 1 to observe LSPI events detailed in their formation process and location in the combustion chamber. To set and control engine-specific parameters, Ford-Werke GmbH provided both experimental institutions with a fully accessible engine control unit (ECU).

The measuring equipment for these investigations included slow and fast data acquisition at both testbed locations. The slow data were recorded by the respective testbed system. The fast data acquisition recorded the indication data and was used to store combustion anomalies like pre-ignitions automatically.

2.2 Pre-ignitions evaluation

In gasoline engines, different combustion anomalies can be detected. In Figure 2, the most common combustion anomalies are shown in comparison to regular combustion. The orange cylinder pressure curve in Figure 2-1 represents a knocking combustion and the black curve shows a pre-igniting combustion cycle. Compared to regular combustion, the energy release of the pre-ignition is shifted forward. The maximum cylinder pressure of pre-ignitions reaches a higher level compared to regular combustion. The challenge was to find a methodology to detect pre-ignitions and differentiate them from other combustion anomalies.

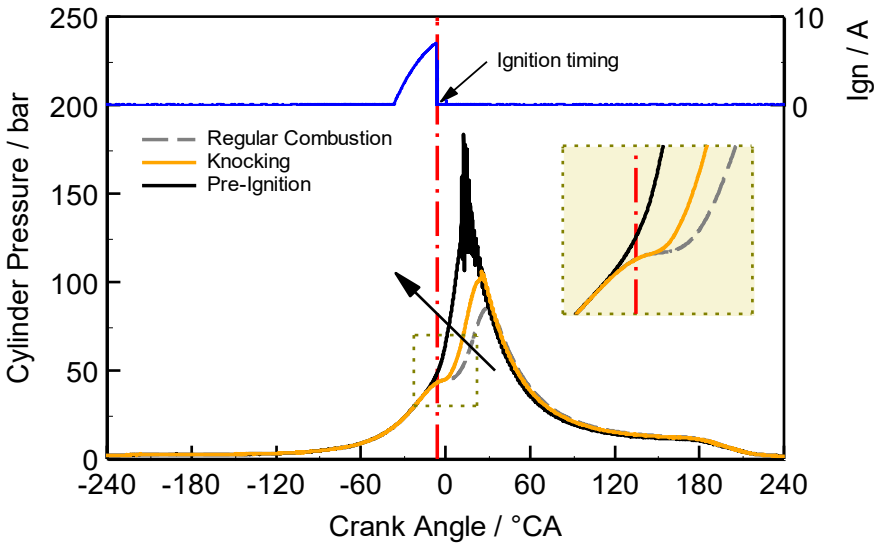

Figure 2-1: Comparison of combustion anomalies.

In order to detect all LSPI events reliable during the measurements, an automated detection function based on the maximum cylinder pressure was used. The indication system, which is able to observe combustion relevant parameters online, automatically stored the combustion anomalies, including their pre- and post-history engine-cycle-based. With this function, all combustion cycles, which exceed an input value of cylinder pressure, were stored automatically.

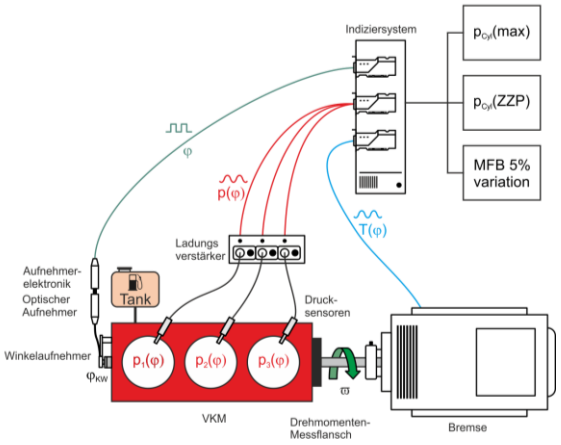

Figure 2-2: Automated pre-ignition detection.

Figure 2-2 shows a schematic of the indication system. The stored combustion anomalies run through an algorithm to separate pre-ignition from knocking events afterward. The evaluation method based on the detection of outliers in the recorded cycles is illustrated in Figure 2-3. With this evaluation, the parameters maximum cylinder pressure p_{cyl}(max), mass fraction burned of 5% MFB5% and cylinder pressure at ignition p_{cyl}(IGN) have been investigated. The stored cycle history has been statistically evaluated. We have assumed the borderline for the detection of outliers for these parameters with $\mu+3\sigma$ related to the normal distribution. If two of the three criteria for a combustion cycle were outliers, the combustion cycle was counted as LSPI event.

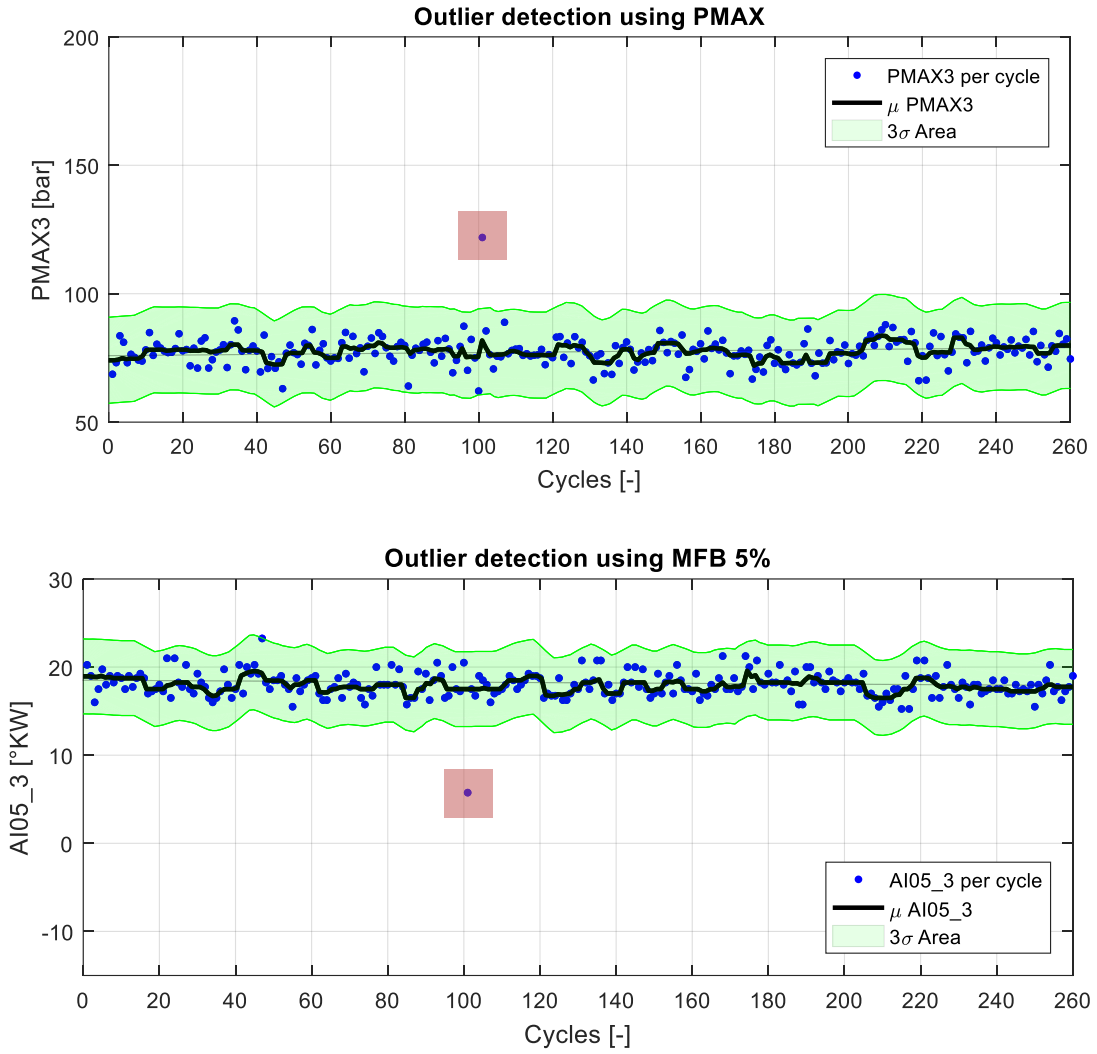

Figure 2-3: Post processing for pre-ignition cycles.

3 Thermodynamic LSPI characterizations

The first work package includes a thermodynamic parameter variation. With these variations, a thermodynamic parameter setting with a relatively constant and reproducible number of pre-ignitions during a test sequence should be found. For the variation, we have investigated the influence of the parameters below on their effect on the occurrence of low-speed pre-ignitions.

- engine speed
- engine load
- start of ignition
- intake air temperature
- coolant temperature
- fuel temperature
- injection pressure

In addition, we have used two different engine fuels, standard RON 95 and Coryton high LSPI fuel, as well as two engine oils, Fuchs 5W-20 and 5W-30, to define the engine liquids for the entire project at the beginning of the experimental investigations.

For the parameter variation, we have defined a number of cycles, which have to be measured in an LSPI test run. Depending on the engine speed, the measuring time has been adjusted to measure a

cycle number of 30 000 cycles which results in a specific measurement time for the investigated engine speeds during the parameter variation. Before we have started the measurement sequence for each parameter variation, a conditioning phase to 10 minutes has been executed. During this conditioning phase, the ignition was changed to a slightly knocking combustion to remove residuals in the combustion chamber. Afterward, the LSPI test was performed under the specified operating conditions. The goal of these investigations was to determine the independence of different thermodynamic boundary conditions on the occurrence of LSPI events. For this purpose, one thermodynamic parameter has been changed for each variation run.

A variation of the coolant temperature in Figure 3-1 shows the already observed behavior regarding pre-ignitions [2]. With an increase in the coolant inlet temperature, the number of observed LSPI events decreased. The elevated pre-ignition frequency with increasing engine speed can be explained with the increased charge motion and piston speed.

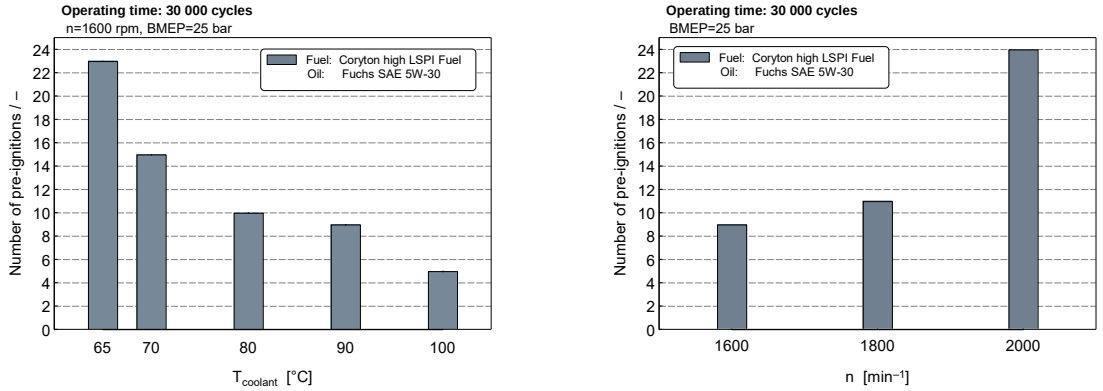

Figure 3-1: Variation of coolant temperature and engine speed.

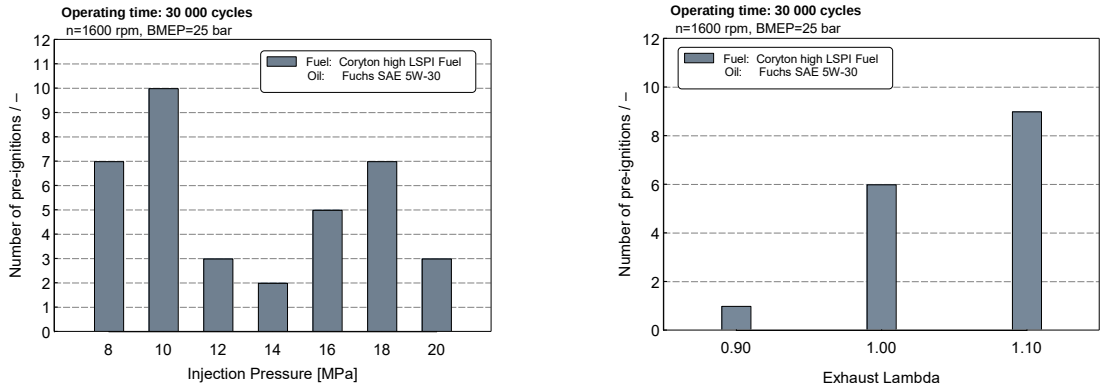

Figure 3-2: Variation of injection pressure and exhaust lambda.

The variation of injection pressure did not show a clear trend. The highest number of pre-ignitions occurred at an injection pressure of 100 bar. A variation of exhaust lambda showed an increasing number of pre-ignitions with increasing lambda. We have to mention here that the exhaust lambda is not equal to the lambda in the combustion chamber. The simulation showed a mean lambda in the combustion chamber lower than 1 for an exhaust lambda of 1.1.

The suspected mechanism on how pre-ignitions occur in this engine at this specific operating point can be explained by an interaction between the injection spray with the liner wall as well as the piston crevice.

Nearly all parameter variations with an assumed worse mixture formation showed an increase in the number of pre-ignitions. For example, a colder cylinder liner wall promotes the condensation of the fuel on the liner wall. This condensation leads to a higher fuel content on the liner wall, which increases the dissolution of fuel in the engine oil. Analytics of the engine oil also showed a high value of oil dilution after parameter variation with worse mixture formation.

As a result of the parameter variation, the so-called ISO operation point has been defined for further investigations. Therefore, limitations regarding the optical investigations have been considered. We have tried to choose a parameter setting with sufficient reproducibility and a sufficient number of pre-ignitions during the first minutes of the LSPI test run. For further optical investigations in Karlsruhe as well as CFD simulations, the following thermodynamic parameter settings were used.

Table 3-1: ISO parameter setting.

ISO OPERATING POINT	
Engine speed	1600 rpm
Engine torque	200 Nm (25 bar BMEP)
Start of injection	250 °CA BTDC
Ignition	- 4 °CA BTDC
Injection pressure	10 MPa
Exhaust lambda	1.08
Coolant temperature	65 °C
Intake temperature	40 °C
Oil	Fuchs Titan Supersyn F EcoDT 5W-30
Fuel	LSPI Fuel

4 Optical LSPI characterizations

Distinctive behavior

All recorded pre-ignition events showed general, unmistakable behaviors. We observe a dynamic deposit build-up at the bore top/ piston crevice area. The most dominant deposit area is to be found in the pool fire region. These deposits build up in a rapid fashion and can get detached by pre-ignition events, especially with heavy knocking ("cleaning effect"). Figure 4-1 does show the deposition pattern after individual optical pre-ignition runs.

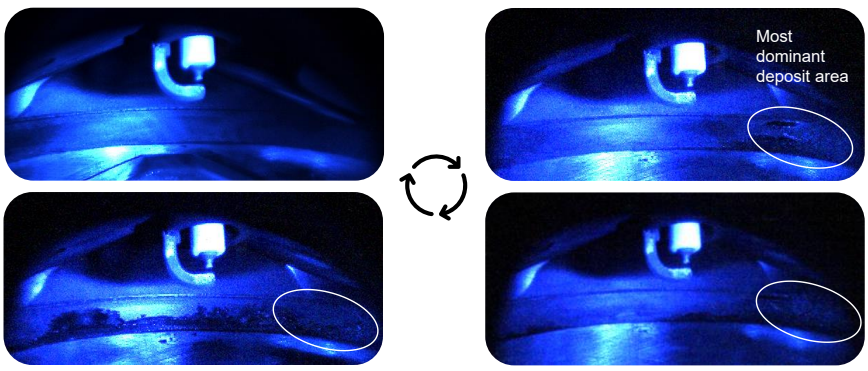

Figure 4-1: Dynamic deposit build-up at PI load points.

Figure 4-2 shows the typical course of a singular pre-ignition event. In the cycle before the pre-ignition initiation, the typical combustion pattern with a strong pool-fire presence is shown. Partly moving solid

particulate matter (particles) of various sizes can be observed in the combustion chamber at regular cycles. The solid property can be attributed to the injection jet impulse transfer without form changing. The pre-ignition is initiated by a glowing solid particulate matter emerging from the piston crevice near the top dead center, which initiates flame propagation near the piston head. In the expansion stroke of the pre-ignition cycle, the process of particle detachment from specific spray/ liner interaction areas can be detected. There is also a luminance-dominated combustion behavior at the piston edge, which indicates an increased accumulation of oil and fuel. Some of these initially burning particles survive the subsequent charge exchange and can still be recognized in the subsequent cycle. The bouncing of a glowing particle on the spark plug base electrode without form changing in the exhaust stroke illustrates the solid substance of these detached particles. The majority of pre-ignition events consisted of individual pre-ignitions.

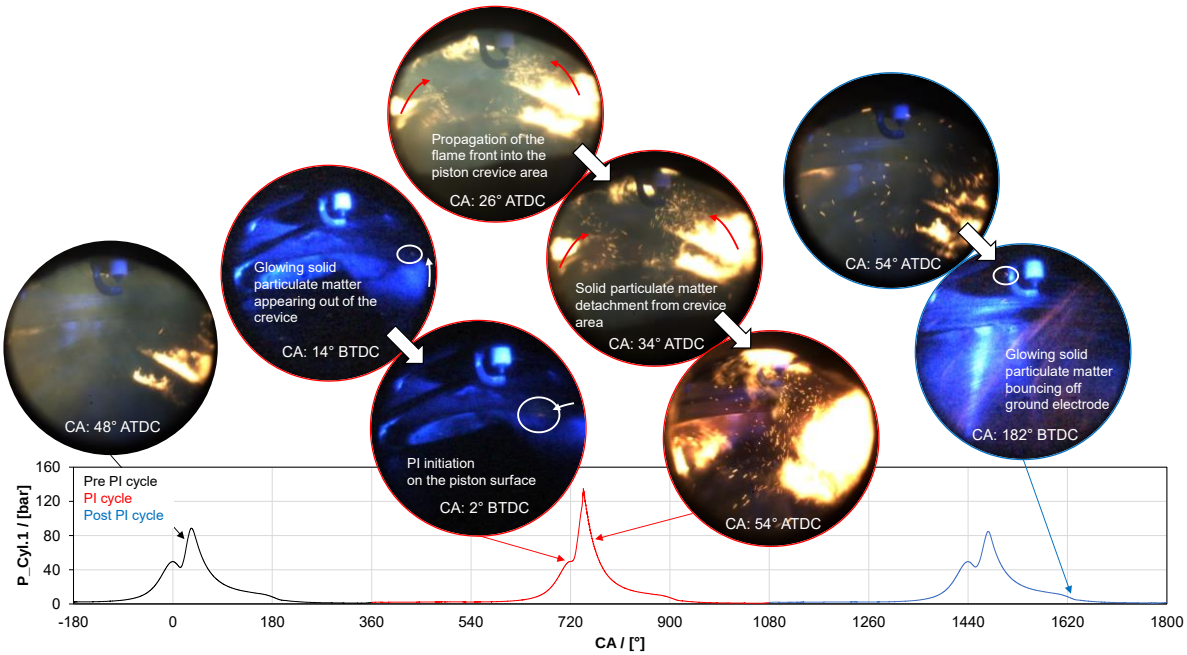

Figure 4-2: Typical course of a single pre-ignition.

In addition to single pre-ignition events, there were also "classic" pre-ignition series. Probably due to the strong scavenging effect, this mainly resulted in series of two pre-ignitions. A representative example is shown in Figure 4-3. The initial pre-ignition is initiated by a glowing particle following the tumble flow. The start of glow likely occurs during compression. After a rebound and at the inlet valve, the air-fuel mixture is ignited near the spark plug. In the following cycle, a large number of burning and glowing particles can be seen during combustion and expansion. These obviously have survived the charge exchange and do not yet seem to have the potential to trigger a further pre-ignition in the compression stroke. Only in the next but one cycle is the repeated initiation of a pre-ignition visible through a particle that begins to glow in the compression stroke. The pure number of particles is no guarantee for the generation of pre-ignition, but it explains the increased occurrence of more than one ignition nucleus during subsequent pre-ignitions. This pattern speaks for the influence of an oxidative process, which in turn is influenced by the combustion air-fuel ratio.

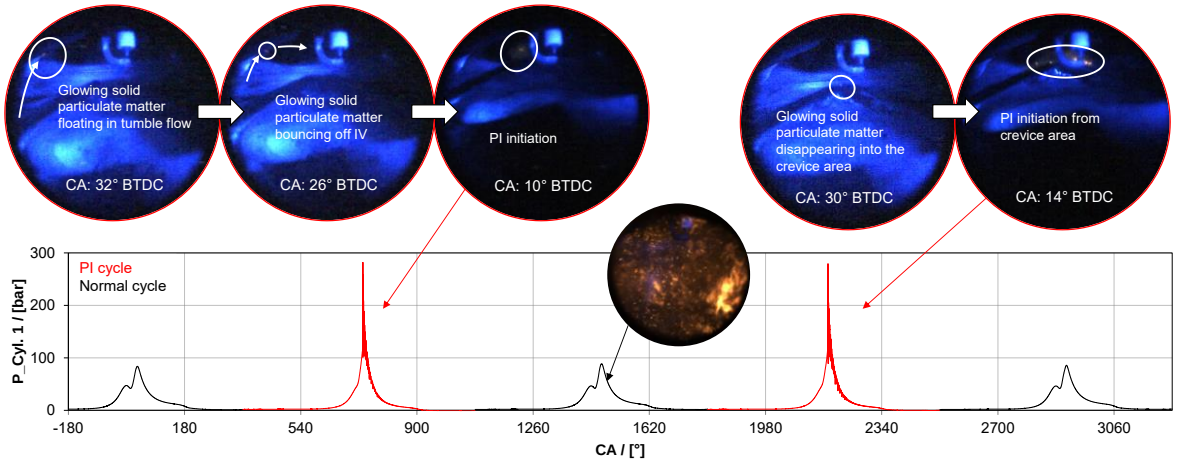

Figure 4-3: Typical course of a short pre-ignition series.

The rare form of an extremely long pre-ignition series shown in Figure 4-4 illustrates the general challenge of pressure-based pre-ignition detection and thus the statistics-driven thermodynamic pre-ignition interpretation. Pre-ignition events can occur which are not detectable by means of a pressure signal. In the event shown, these correspond to the first 13 cycles. There is a constant ignition source on a deposition point on the piston at the pool fire area (most dominant deposit point), which is only stopped by the occurrence of the pre-ignition event **1** with two initiation sources. The resulting greater pressure amplitudes suggest a sudden release of this critical deposition component. The picture resulting from **2** shows a congruent characteristic to Figure 4-3.

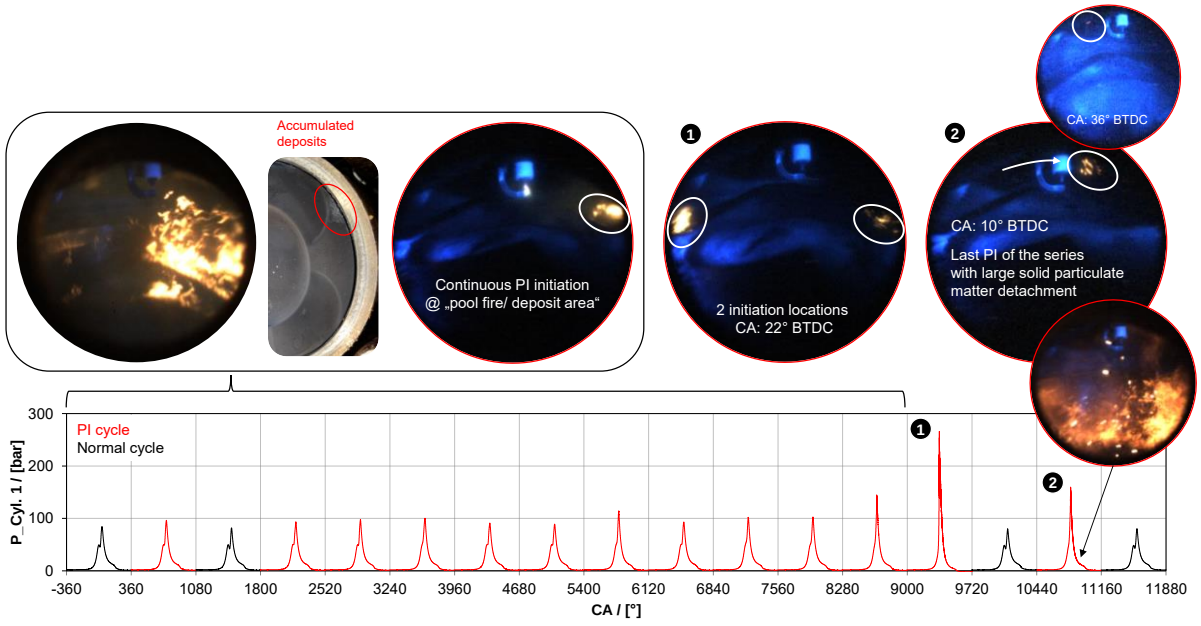

Figure 4-4: Typical course of a very long pre-ignition series.

Initiating mechanism synthesis

Figure 4-5 shows the overview of the evidence-based pre-ignition formation observations synthesized from all optical pre-ignition characterizations. **1** shows the start of glowing of a small moving particle near the top dead center. The later pre-ignition initiating glowing particle 14° CA BTDC is, however, much larger. This leads to the conclusion that particles must have a minimum size in order to have the

potential to trigger a pre-ignition. Since the image details in **1** are an observation period of a subsequent pre-ignition, a large number of particles are present in the combustion chamber at this point in time. The fact that only two of these particles are detected glowing in the observation volume causes the assumption of different specific particle properties. A purely morphological effect seems to be unlikely here, which is why it is presumably a different material composition. There seem to be different reactivities of individual particles.

The image details from **2** confirm the assumption of solid substances that cause pre-ignition. This is confirmed by the ability of the particles to bounce off the inlet valve without changing their shape. The shown particle detachment from specific deposition areas (pool fire area) shows the interrelationship between the formation of deposits and the appearance of particles in the combustion chamber.

3 shows a glowing particle in the intake stroke of a single pre-ignition cycle with no pre-ignition history. The fact that there is a glowing particle here despite the cool combustion chamber conditions deepens the assumption that the particles have to be reactive. The activation conditions for this reactive process must have been set in the combustion process of the previous cycle. The strong observed air-fuel ratio influence on the pre-ignition frequency is presumably also evident here. This must have the opposite effect. On the one hand, sub-stoichiometric combustion increases the formation of deposits, and on the other hand, available oxygen during combustion offers the possibility of setting oxidative activation conditions for particles.

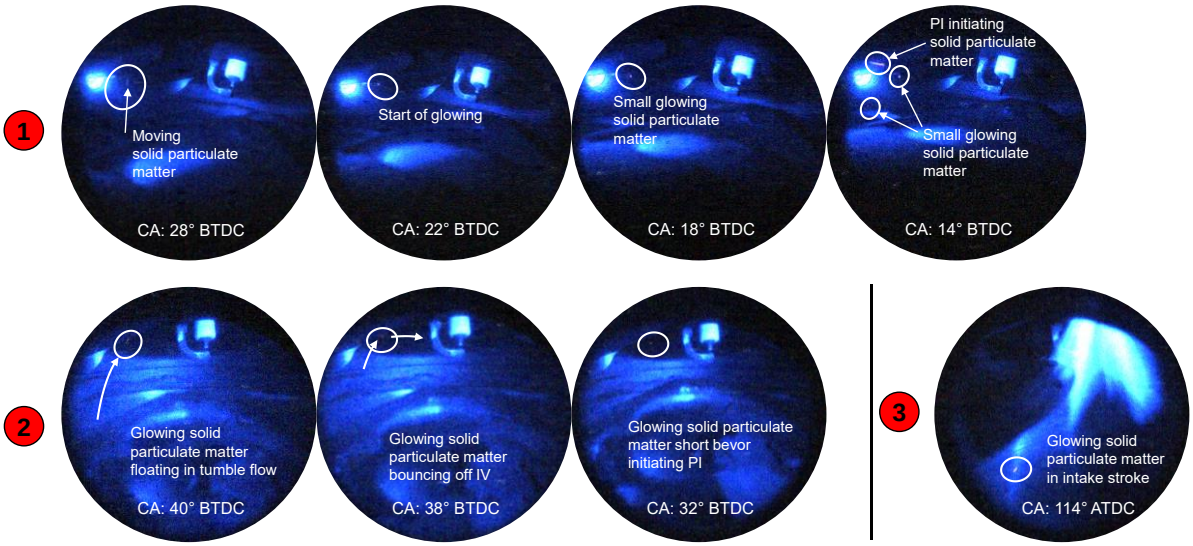

Figure 4-5: Solid particulate matter pre-ignition initiation characteristics.

The evaluations of the previous pre-ignition characterizations show the picture of a multi-cyclic pre-ignition mechanism, which is defined by (reactive) deposit formation and the release of (reactive) particles. In the following, the simulative validation of the assumptions is presented.

5 Simulative LSPI characterizations

5.1 Mixture Preparation and Wall film analysis

The goal of the simulation was to predict the fuel film formation and mixture preparation at the investigated "ISO-operation point." Therefore, the simulation time could be limited to a single engine-cycle without including the combustion process. The beginning of the simulation was set to 270 °CA to minimize the errors made in the initialization process. The end of the simulation was set to spark timing (724°CA). Special focus was placed on the application of a detailed fuel surrogate model. Therefore, an 11-component fuel surrogate was generated using a 0D-distillation model. In order to account for the mixture effects of the real fluid, the vapor pressure was corrected by calculated activity coefficients (UNIFAC method).[5] The spray model was calibrated using measurement data, shown in Table 5-1.

Table 5-1: Spray measurement data.

Rail pressure	**100 bar**
Ambient pressure	1 bar
Injector mass flow	25.70 kg/h
Penetration length	High speed imaging
PDA (SMD/DV90) - 50 mm distance	13.2 µm / 23.2 µm
Spray coil orientation	Footprint measurement
Spray cone angle (outer/inner)	11° / 0°

The secondary droplet break-up was implemented according to the Reitz-Diwakar model. The droplet-wall interaction was calculated by using the Bai-Gosman impingement model. The turbulent flow field was described with a RANS approach in combination in conjunction with a k-ε RNG turbulence model. Figure 5-1 shows the liquid film distribution in the combustion chamber at EOI. Additionally, the lambda and temperature distribution inside the combustion chamber is shown at three distinct times near TDC.

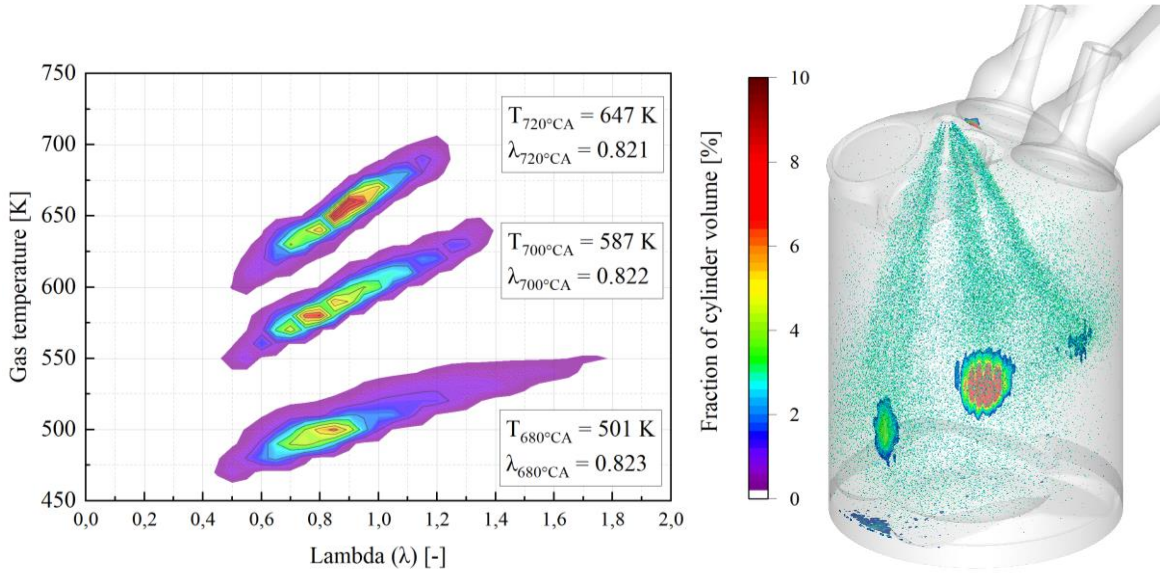

Figure 5-1: (left) In-cylinder lambda and temperature distribution, (right): film distribution at EOI.

The decreasing charge motion velocity toward BDC enables the spray to reach the cylinder liner and the piston surface. The film mass peaks shortly after EOI at 585 °CA aTDCf and decreases afterwards due to evaporation. The majority of the liquid film mass is concentrated at three distinct areas on the

liner and one region on the piston surface. Furthermore, it can be observed that the wetted piston area is underneath a distinct fuel-wetted liner area. These areas are in accordance with the optical observations performed at the testbed.

The heat transfer from the liner walls to the wetted areas is too low to evaporate the film completely. Therefore, the piston wipes off the liquid film during the compression motion. This leads to fuel accumulation in the piston crevice volume, where it survives till the end of the simulation.

The appearance of surviving wall films until spark timing indicates incomplete mixture formation. Figure 1 (left) displays the situation at 680 °CA, 700°CA and TDC. The figure displays the situation at 680 °CA, 700°CA and TDC. In the shown timespan, the mean lambda value of 0.82 remains almost constant. Due to convective and diffusive transport, the rather wide lambda distribution gets narrower towards TDC and ranges from 0.5 to 1.25. The ongoing compression leads to an increase in the mean temperature level. As a result, the temperature difference between the walls and the gas phase increases, which results in a wider temperature band. Although, it has to be mentioned that the temperature bandwidth increases only by 25 K.

Furthermore, it can be observed that the displayed parameters are not completely independent. Fuel-rich areas appear to be colder than lean areas. This is caused by the cooling effect of evaporating fuel droplets. The hottest observed gas temperatures are 705 K at TDC.

5.2 Droplet induced ignition

The optical investigations described in the previous sections suggest LSPI is related to ignition scenarios associated with condensed matter rather than a pure gas-phase phenomenon. Numerical studies were performed to scrutinize different such ignition scenarios and assess their suitability as a cause for LSPI on a theoretical basis.

Simulations are based on a model scenario in which droplets of a reactive substance (representing liquid oil or oil/fuel mixtures) are embedded into an ambient, less reactive fuel/air mixture [6]. The situation is thus characterized by an auto-ignition prone droplet versus the less auto-ignition prone ambiance (Figure 5-1). The description of chemical reactions is based on the reaction scheme from [7].

The question to be answered is then under which conditions does the droplet affect auto-ignition and flame development in the ambient gas. This will depend on the physical conditions of the ambient gas, the droplet substance, and the physical conditions.

5.2.1 What happens at the droplet?

Successful modeling of LSPI requires realistic treatment of phase change, molecular transport, chemical reaction, as well as their mutual interaction. Studies were therefore performed using the Code INSFLA for detailed simulation of reacting flows in transient, inhomogeneous systems [8].

We consider the droplet and ambiance as initially separate entities, which are then brought into contact at time $t = 0$. Several events will then occur and interact. In engine conditions, the ambient temperature will usually exceed the droplet temperature; therefore, there is heat transfer between ambient gas and droplet. This will allow the droplet to evaporate, causing a flux of droplet-originating vapor from the droplet surface into the ambiance. The droplet vapor then mixes with ambient fuel/air; with increasing

distance from the droplet surface, the droplet substance gets diluted with ambient gas. This mixing also affects the temperature field in the vicinity of the droplet.

In this inhomogeneous compositional and thermal field, chemical reactions occur. In contrast to the often-used one-step representative chemical reaction step, in reality, there are multiple elementary reaction steps that occur in sequence or in parallel. This leads to the formation of radicals, chain branching.

While each of the individual elementary processes (heat transfer, evaporation, mixing, chemical reaction) is well understood, the coupled process becomes complicated by the overlap and interaction of these processes. It is thus not solely the individual elementary processes but rather their mutual coupling that renders LSPI such a difficult-to-track problem [9, 10].

5.2.2 Processes during and after droplet ignition

Figure 5-2 shows a typical case of auto-ignition at a droplet by means of spatio-temporal temperature profiles.

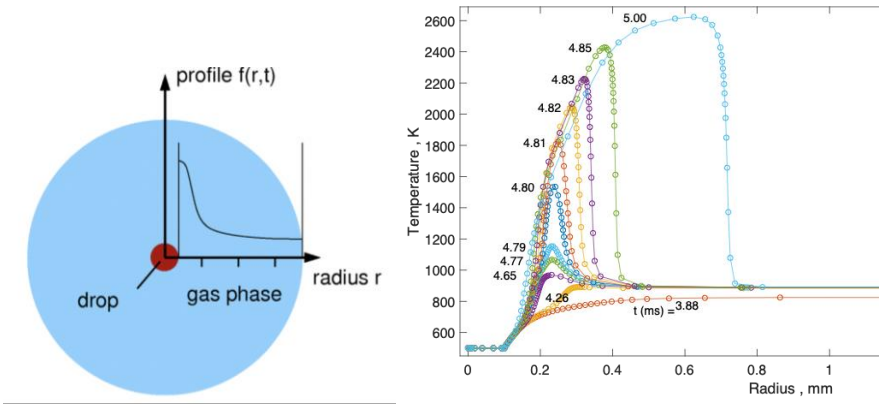

Figure 5-2 Left: Basic Scenario: An (auto-ignition prone) droplet in a fuel/air ambiance [6] Right: Temporal evolution of temperature profiles during the auto-ignition at a droplet with an initial radius 0,1 mm. Numbers near the curves indicate the times (in milliseconds) after exposure of droplet to the gas phase.

At t = 0, the droplet gets exposed to ambient gas. The droplet begins to evaporate, and the released vapor diffuses into the ambient gas phase. The curve corresponding to t=3.88 ms corresponds to the mixing of ambient gas with the vapor released by the droplet. The temperature increases with increasing radius because the ambient gas has a higher temperature than the droplet. After some time, ignition occurs at some distance away from the droplet; this is visible first at the 4.26 ms and 4.65 ms curve. After ignition, a flame starts to spread; this is apparent by the expanding region of high temperature after about 4.85 ms in Figure 5-2. Unlike the example shown here, local ignition need not always lead to flame propagation. An important result is that the ignition can occur some distance away from the droplet. Also, ignition and flame propagation can be separated temporally from the existence of the droplet that has caused the vapor. As a consequence, despite the fact that causality between the vapor releasing droplet and the subsequent ignition/flame propagation clearly exists, there need not be clear observational evidence for this causality.

5.2.3 Droplet Ignition modeling studies

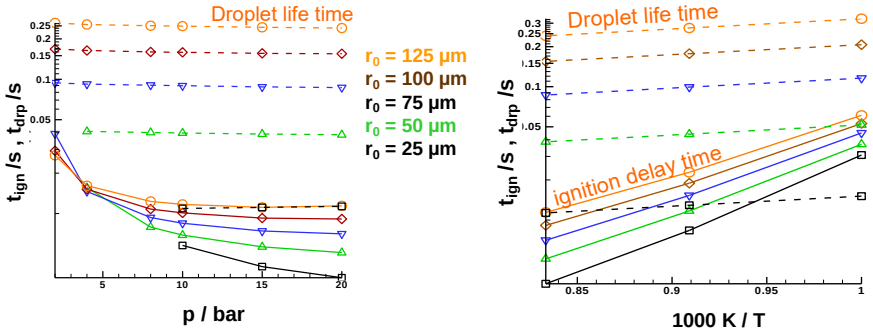

Figure 5-3 Excerpts from a droplet ignition "library ", giving time scales of droplet lifetime (time till droplet has evaporated) and ignition delay as a function of gas-phase temperature (right) and pressure (left).

A large parametric study of droplet ignition cases was performed. All are based on droplets embedded into an iso-octane air ambiance. Multiple simulations were run in a systematic approach to study the influence of several quantities: Gas-phase properties (temperature, pressure, equivalence ratio), droplet properties (initial droplet diameter, initial droplet temperature, droplet composition) on ignition delay times, evaporation rates and droplet lifetimes. Figure 5-3 gives an example of such a study; the extensive data allow to inspect the essential dependencies of the droplet-relevant time scales (droplet lifetime, ignition delay time, mixing times of droplet vapor and ambient gas) and their dependence on physical conditions like temperature, pressure. Importantly, analysis of the results can allow the identification of conditions where droplet ignition is sensitive or insensitive to the change of a parameter.

As an important result of the analysis of the parametric ignition studies shows that for n-heptane droplets in iso-octane/air, LSPI-relevant ignition delay times were seen only at high gas temperatures (> 740 K).

5.2.4 Robustness of results with respect to kinetic data

The outcome of models will usually depend on the input data. For simulations of auto-ignition, chemical kinetics data are crucial. Notably, for each of the elementary reaction steps in a reaction mechanism, the values of the Arrhenius parameters describing the speed of chemical reactions can have a significant influence.

To study how strongly the data of an ignition depend on the kinetic parameters, these were "tuned" slightly, and simulations were repeated with the tuned reaction kinetics data to assess the change of ignition delay times with respect to the "unperturbed" data. The range of the tuning was chosen within the limits of the uncertainty of kinetic data.

5.2.5 Robustness of results with respect to oil composition

A possible source of uncertainty stems from the fact that droplet material might not consist exclusively of straight-chain hydrocarbons (of which n-heptane is a representative and which are among the fastest igniting hydrocarbons). As a plausible scenario, one may consider reacting components in the droplet, which display even faster ignition. A prominent class of such components is the Keto-hydroperoxides, a family of partially oxidized hydrocarbons. These substances might form from radical recombination reactions when hydrocarbons are exposed to the high-temperature environment of engines [11, 12].

Studies of droplets that were "doped" with different kinds of keto-hydroperoxides were performed to assess how the more reactive species would accelerate the ignition.

Figure 5-4 shows the result of such a study. Relative to the case of a pure n-heptane droplet at the same initial conditions, keto-hydroperoxides can accelerate the auto-ignition (and flame initiation). However, even with these reactive substances, ignition delay times are too long to explain LSPI, if temperatures remain below about 740 K. At these temperatures (at engine-relevant pressures), chemical kinetics with these substances is too slow to explain LSPI under the studied engine conditions.

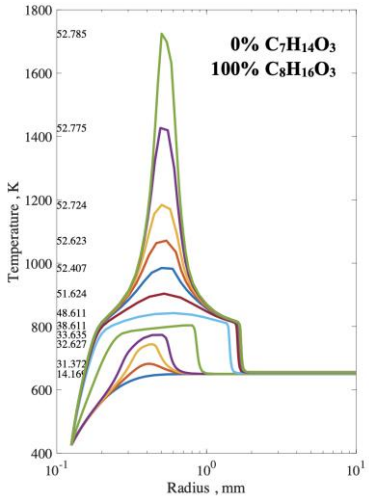

Figure 5-4 Temperature profiles during auto-ignition of a keto-hydroperoxide droplet. Numbers indicate the time represented by each curve.

The model studies, which assume a straight-chain hydrocarbon (n-heptane as a proxy) or keto-hydroperoxide ($C_7H_{14}O_3$ and $C_8H_{14}O_3$) in the droplet and iso-octane/air in the surrounding gas phase, predict long ignition delay times for these scenarios. Faster ignition is possible if the influence of additional substances on chemical kinetics is postulated.

Such substances may be formed by an operating engine, if not in a single cycle, then in a sequence of consecutive cycles where there is an accumulation of chemical progress. The pattern is that the "fresh" hydrocarbon forms radicals in one cycle, which recombine in "colder" regions of the combustion chamber, forming intermediate species. Some of them are potential "superfast" (in the sense of auto-ignition delay times) substances. They may survive a combustion cycle and also the gas-exchange phase, e.g., in cold crevices. Over several cycles, this can lead to an accumulation of highly reacting substances.

The detailed treatment of this is the subject of further studies; our simulations from an earlier research project already hinted at the plausibility of such a scenario, shown exemplarily in Figure 5-5.

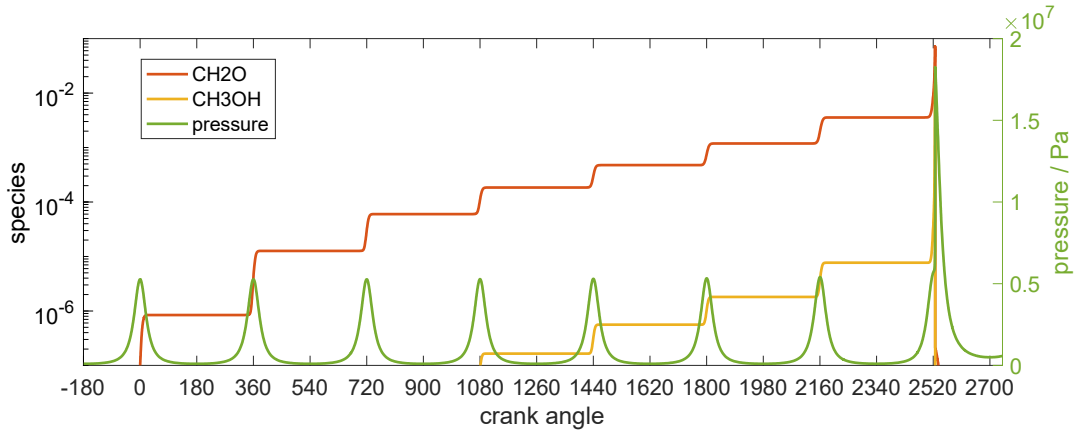

Figure 5-5 Result of a detailed chemistry simulation showing the consecutive build-up of intermediate species from an initial hydrocarbon/air mixture between subsequent engine cycles. Only at the 8th compression, the formed intermediates lead to auto-ignition. Note the log scale of species: During most cycles, the amount of intermediates is negligibly small; the exponential growth "strikes "at the 8th cycle, where an auto-ignition event occurs.

5.3 Hot particle induced ignition

Besides oil-fuel droplets, detached particles are assumed to be a potential root-cause of pre-ignitions. In order to determine the gas-phase ignition potential caused by a hot particle inside the combustion chamber, a detailed sub-model of a single particle had to be established.

Whereas oil-fuel droplets accelerate ignition processes by evaporating reactive species, particles induce an ignition by heat transfer. The particles inside a cylinder are heated up by regular combustion cycles. Moreover, the particle itself could increase the surface temperature by exothermal reactions. Since the composition and the reactivity of such detached particles are unknown, the hot particle was simplified as a hot surface. Only the heat transferred from the particle surface to the reactive gas-phase environment was considered. The general advantage of this modeling approach is that it is valid for reactive and non-reactive particles. Figure 5-6 shows the numerical grid used in this sub-model.

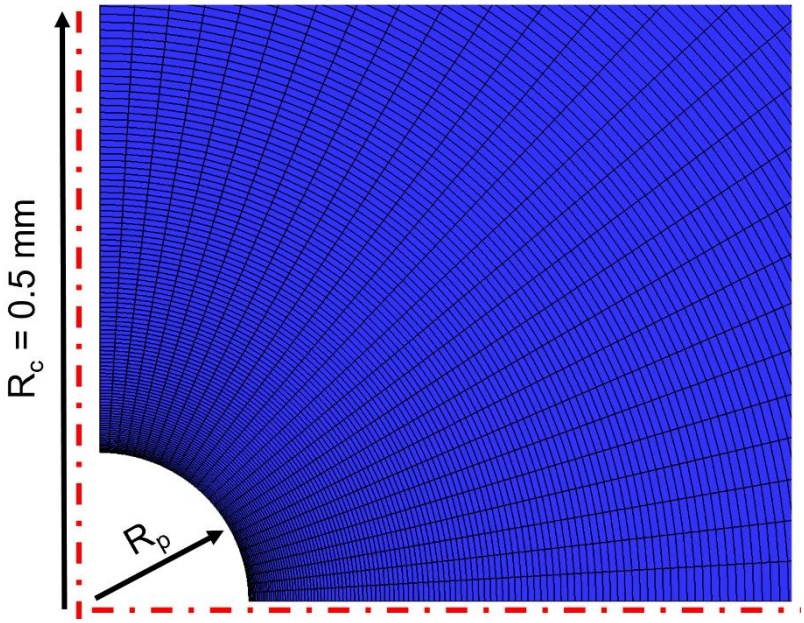

Figure 5-6: Hot particle ignition sub-model.

A two-dimensional structured radial grid was set up to model the heat transfer problem numerically. Double symmetry conditions were used to reduce the model size to a 90° sector. The overall simulation

domain was limited to a radius of 3.125 mm discretized with 8,100 cells (dR x dφ x dz = 300 x 27 x 1). The particle radius (Rp) is set to 125 µm, which represents the typical size of the piston crevice gap. In order to capture the sharp increase of the gas temperature near the hot surface, the boundary layer had to be resolved. Therefore, the cell size at the wall was set to 1 µm. Towards the outer end of the simulation domain, the cell size increased to 20 µm using a stretching factor.

The gas-phase was modeled as a mixture of air (76.8 %-m/m N2, 23.2 %-m/m O2) and fuel. The fuel was represented as a TRF-surrogate. The mixture composition is defined by applying the "modified linear-by-volume" method of Morgan et al.[13] Table 5-2 shows the TRF-surrogate composition.

Table 5-2: TRF representation of fuel.

Fuel measurement	**Value [-]**
RON	96.5
MON	86.0
Surrogate species	**Mass fraction [-]**
iso-Octane	0.1246
n-Heptane	0.1565
Toluene	0.7189

In analogy to the droplet ignition investigations, the chemical reaction kinetics were calculated in the gas phase using the same semi-detailed TRF mechanism. The ignition delay time is defined as the time elapsed until an established flame front passed through a critical radius of 0.5 mm. The critical radius was set according to Kalghatgi et al.[14], who published the critical radius for n-heptane/air mixtures.

In order to use the hot particle-induced ignition model under transient conditions in the framework of a CFD simulation, a set of pre-calculated cases are used to generate a 4D ignition delay map. Additionally, an ignition-integral approach is introduced in analogy to the well-known Livengood-Wu knock integral, shown in equation 1.[15] The parameter range of the 4D look-up table is based on the performed CFD simulation of mixture preparation and wall film formation. Additionally, a wide range of different particle temperatures was used, shown in Table 5-3.

$$\tau_{ign} = \sum_{i=1}^{N} \left(\frac{\Delta t_{TS,\,i}}{\tau_{ign,\,i}\,(T_p,\,T_G,\,p_G,\,\lambda)} \right) \tag{1}$$

Table 5-3: Parameter set of the pre-calculated cases.

Parameter	**# Variations**	**Used values**
Gas temperature	4	500 K, 575 K, 650 K, 725 K
Gas pressure	3	10 bar, 30 bar, 50 bar
Lambda – TRF	4	0.5, 0.8, 1.0, 1.2
Particle temperature	7	1000 K, 1200 K, 1300 K, 1400 K, 1500 K, 1600 K, 2000 K

Applying this model to mean in-cylinder conditions, a minimum necessary constant particle temperature of 1167 K could be found to initiate an ignition at spark timing. This value holds true if the particle is released at IVC. Figure 5-7 shows the results achieved for a variety of release and ignition timings.

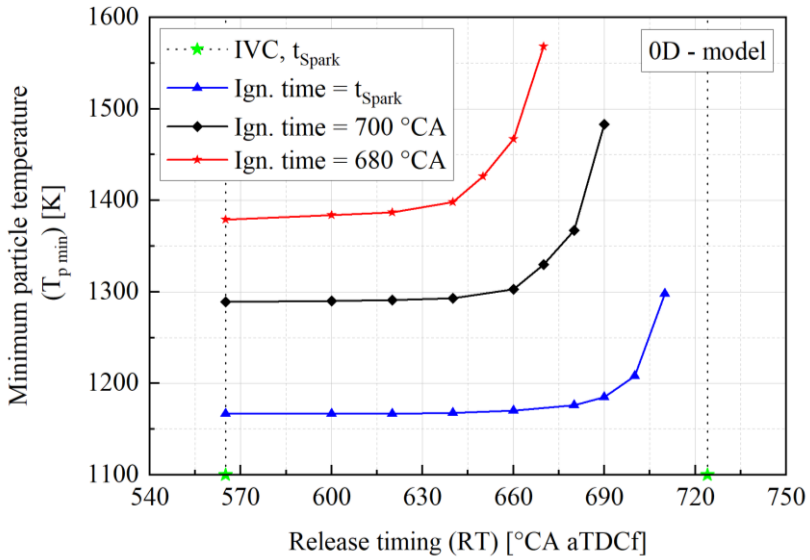

Figure 5-7: Release and ignition timing sensitivity.

The blue curve displays the results achieved by delaying the release time of the particle while maintaining the ignition timing. It clearly shows the minor impact of the early compression phase on the ignition timing. However, the requirement of an earlier ignition increases the necessary particle temperature significantly.

Since the thermodynamic conditions inside the combustion chamber are inhomogeneous to some extent, a stochastic particle release CFD model was established to capture statistical particle histories inside the combustion chamber. The particles were initialized at the piston crevice section, where pronounced fuel wall wetting occurred. The initial particle properties are based upon optical observations and are summarized in Table 5-4. Figure 5-8 shows the particle temperature history of all 10.000 released particles during two engine cycles.

Table 5-4: Summary of particle properties.

Parameter	Unit	Used value	Reference
Release time	°CA aTDCf	680	Optical observation (earliest observed timing)
Initial Speed	m/s	1 – 7.5	Optical observation
Initial particle temperature	K	462.5	Assumption (avg piston/Liner)
Diameter classes	µm	100, 200, 300, 400, 500	Engine geometry and optical resolution
Released particle count	#	10.000 (2.000 each diameter class)	
Thermal mass ($\boldsymbol{\rho * c_p}$)	kJ/m³K	1000	[16]
Density	Kg/m³	1800	[17, 18]
Conductivity	W/mK	1.06	[16]

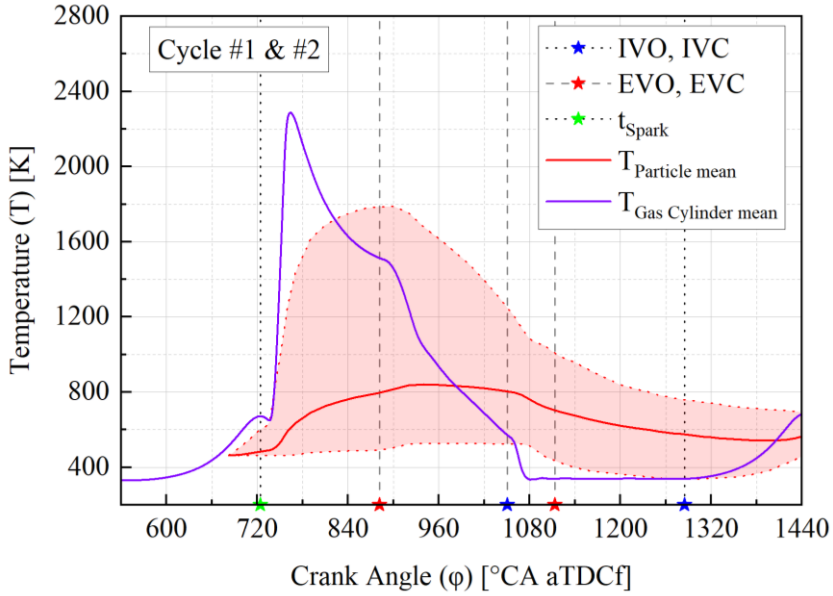

Figure 5-8: Particle temperature history considering engine cycle #1 and #2.

The solid red line represents the mean particle temperature. Additionally, the minimum and maximum values of the particle temperatures are shown. It can be noticed that the mean particle temperature does not increase significantly during the initial cycle (#1). However, the smallest particles are able to increase their temperature up to ~600 K.

With respect to the follow-up cycle, the particles are heated up during the combustion phase. The hottest particles reach a temperature of ~1200 K at IVO. The fresh intake air cools down the particles again. Therefore, the maximum particle temperature is decreased during the following compression phase and falls below 800 K.

As a result, the ignition-integral model predicts no ignition in both engine cycles. This leads to the conclusion that particles that are able to initiate a pre-ignition in the follow-up cycle and especially in the initial cycle have to be reactive. Otherwise, the surface temperatures will not be sufficient. The rate of heat release (reactivity) of such detached particles is currently unknown. Especially, the influence of inorganic residues from oil additives (Ca, Mg, Zn, Mo, …) is assumed to have a major impact. [19]

6 Key experiments

To further establish the mechanism, the results of the specific key experiments carried out are presented below.

6.1 LIF detection of engine fluids

LIF fuel detection

In the CFD simulations, specific locations of fuel film applications on the liner could be analyzed in the "ISO load point." These could not be localized under high-speed boundary conditions during engine operation due to the short exposure time and the resulting relatively weak fluorescence signal, as well as the increasing access window fouling. For this reason, the fuel fluorescence image was taken under a longer exposure time after an "emergency stop" of the engine from the "ISO load point." The result and the CFD and deposition correlations are shown in Figure 6-1. The fluorescence image after the

engine emergency stop shows a clearly inhomogeneous fuel accumulation image in the area of the bore top/ piston crevice. The specific attachment points correlate well with the liner wetting points occurring in the spray and liquid film simulation in the "ISO load point." A correlation can also be found in the deposition image (**1**, **2**, **3**). In the simulation, point **2** shows the largest amount of fuel applied to the liner, which corresponds to the "dominant" crevice deposit point. The specific deposit point found on the piston at the position of the constant pre-ignition initiation (pool fire area) from the extremely long pre-ignition series (**4**) correlates with the CFD fuel piston wetting point.

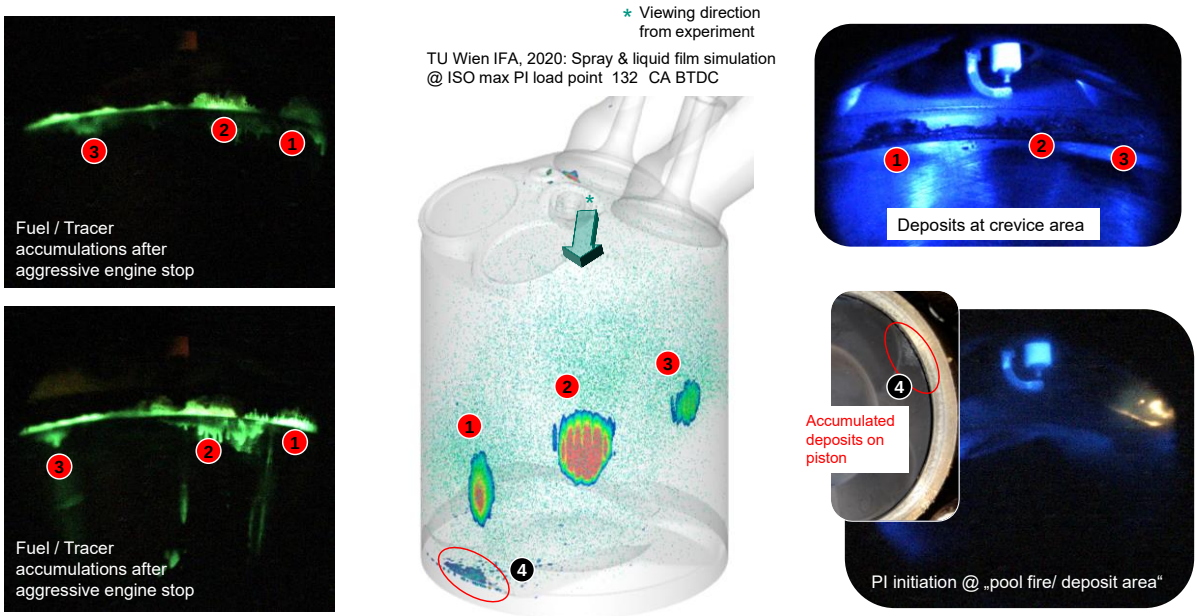

Figure 6-1: Experiment / CFD correlation of fuel liner interaction and deposit build-up.

LIF oil detection

The detection of oil drops during engine operation proved to be very challenging. This is due, among other things, to the general optical limitations of LIF operation on the real engine system and the operating conditions under full load. In direct comparison to fuel fluorescence, oil shows significantly worse optical properties (light penetration) as well as a poorer tracer concentration potential. For these reasons, no oil fluorescence could be detected with either tracer (Lumilux CD345 and PM567A) in normal "ISO load point" cycles. However, the hypothesis described in [20, 21] of the ejection of oil-containing droplets in the case of a super-knocking event with detonation waves could be included in Figure 6-2 and thus confirmed. In particular, this can lead to further particle generation and thus contribute to the development of subsequent pre-ignitions. In this specific case, 256 mg of Lumilux CD345 was used for 4.2 liters of Fuchs 5W30.

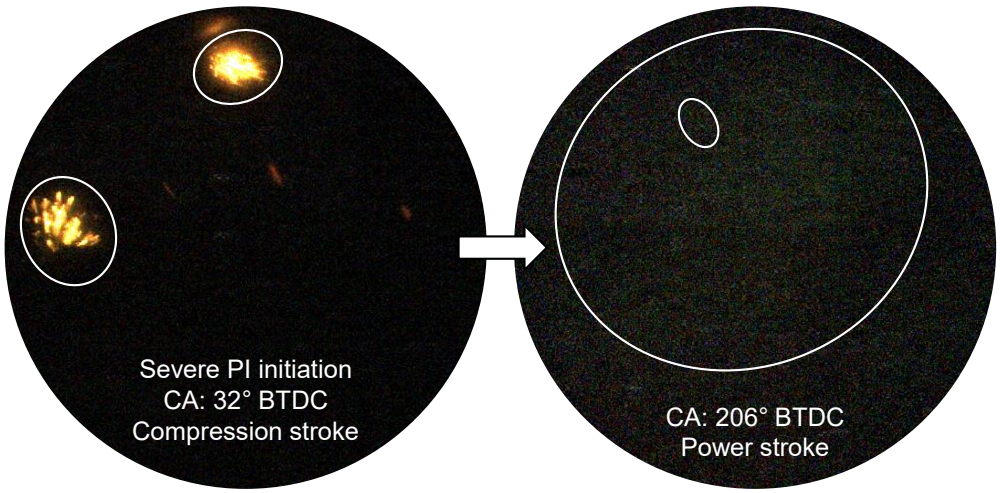

Figure 6-2: Detaching oil droplets by pre-ignition.

6.2 CNG engine operation and oil injection

The investigations with CNG as fuel were not performed at the operation point of the parameter variations. We had to increase the engine speed for the CNG investigations in comparison to the ISO operating point from 1600 rpm to 1850 rpm to reach the goal torque of 200 Nm.

The idea behind the CNG investigations was to exclude the interaction between the injection spray and the liner. The investigations with CNG as fuel confirmed the assumptions about the necessary attendance of residuals in the combustion chamber to gain pre-ignitions.

In the base investigation point, during 5 tests, no pre-ignition occurred. To demonstrate the influence of residuals in the combustion chamber, we also set up an injection method at the CNG investigations. We were only able to measure pre-ignitions with an oil quantity of 2 g/min. All other investigations showed no combustion anomalies. Figure 6-3 shows the CNG findings compared to the CNG operating point with standard gasoline injection.

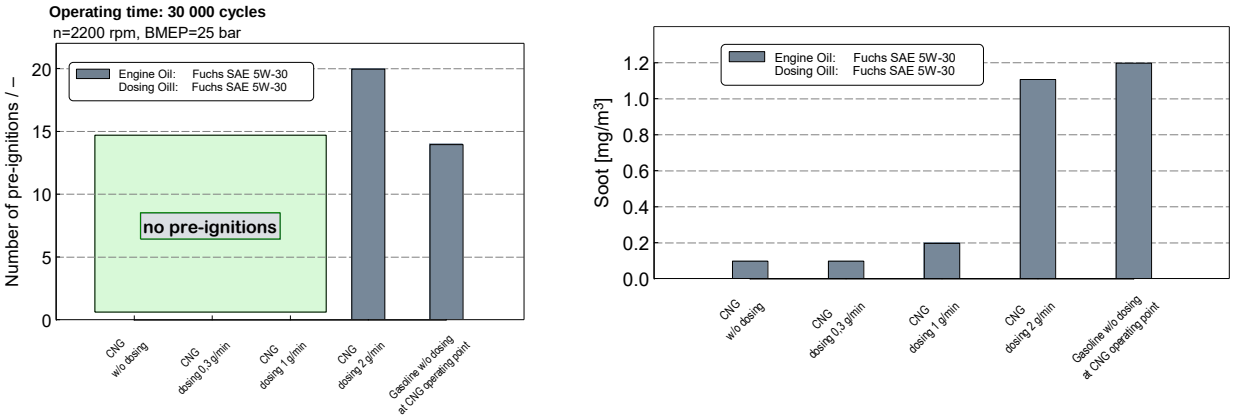

Figure 6-3: CNG investigations and soot values.

6.3 Optical Oil injection investigations

Different oil properties showed a significant influence in the thermodynamic pre-ignition characterization. In order to better understand the role of the engine oil in the pre-ignition mechanism, the effects of an additional oil introduction into the combustion chamber at different load points were investigated. A strong influence on the pre-ignition process was found, which is to be expected. The pre-ignition frequency increases strongly depending on the amount of oil injected. The load area in which pre-ignition occurs also expands strongly downwards. There is a frequent occurrence of relatively mild pre-ignitions. The introduction of oil via the inlet valve 2 of the first cylinder results in the characteristic shown in Figure 6-4. Among other things, there is a specific deposit formation at the exhaust valve 2 opposite the oil inlet. This could be correlated by means of LIF oil droplet tracking with an oil droplet movement path in the cylinder at the "ISO load point" as well as a pre-ignition initiation by a deposit surface ignition at the exhaust valve. The pronounced scavenging effect explains the special movement path. For a clearer representation, the oil drop representations are inverted grayscale images derived from the original images. The deposits created in this way serve as reference deposits in the further course of deposit characterization. All optical results refer to an injected oil mass flow of 0.35 g/min Fuchs 5W30.

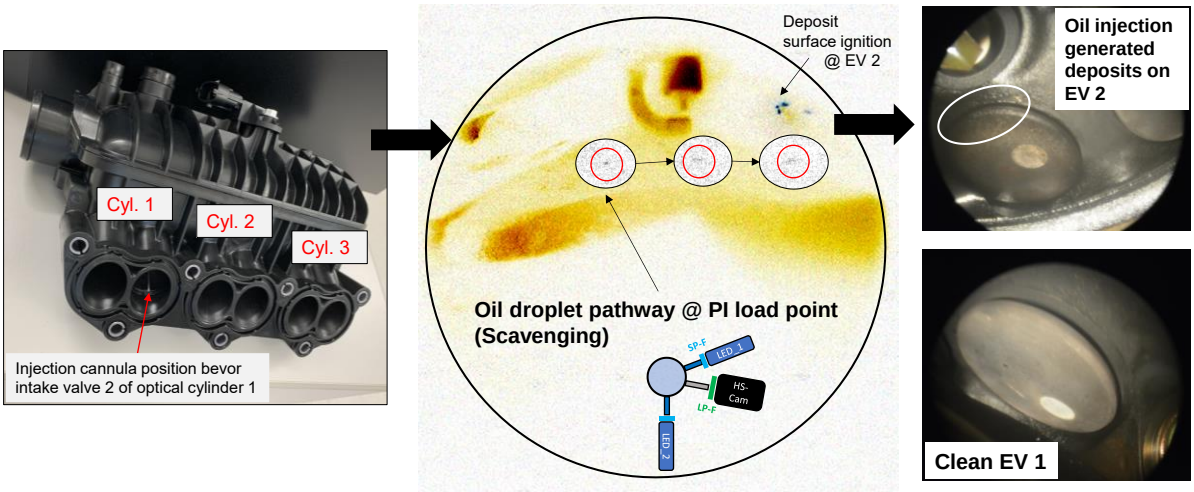

Figure 6-4: Oil path in combustion chamber at PI load point with correlated deposit place.

A direct optical pre-ignition comparison shows a clear difference in the initiation characteristics. Figure 6-5 summarizes the key elements.

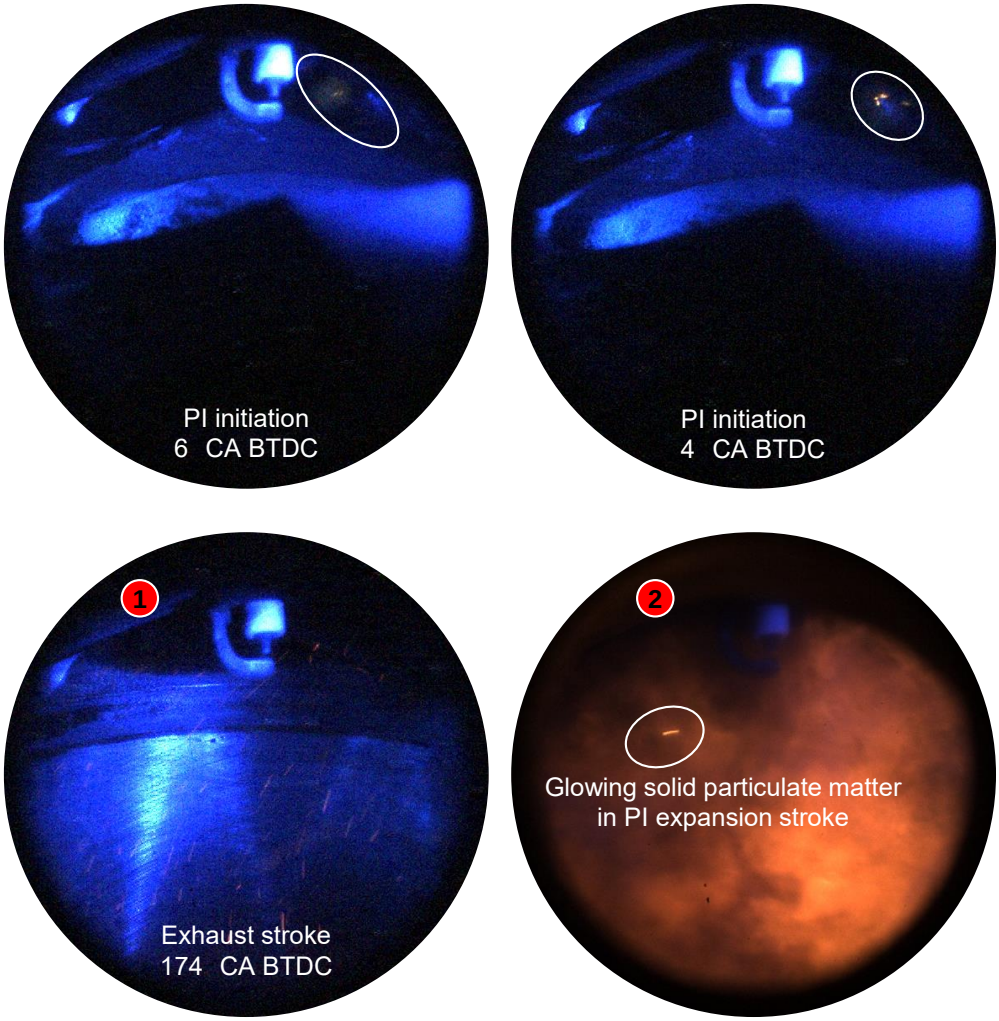

Figure 6-5: Oil injection pre-ignition characteristic.

The majority of all pre-ignitions generated are due to deposit surface ignition at the exhaust valve 2. Oil droplet ignition could not be observed. The fact that each pre-ignition generation requires a temporal oil injection lead time gives indications of necessary conversion processes in the form of deposit formation. In addition to the surface ignitions, there were also isolated cases of the well-known pre-ignition initiations by glowing particles. **2** shows a large glowing particle in the expansion phase of a pre-ignition. Here, the oxygen content in the residual gas must have an effect on the particle oxidation process. The strong influence of the air-fuel ratio on the pre-ignition rate also supports this assumption. **1** shows the increased presence of glowing particles in the exhaust stroke after pre-ignition compared to the optical characterizations without oil injection. This suggests a larger proportion of reactive particles/deposits, which in turn, along with the additional deposits, is an explanation for the greatly increased pre-ignition occurrence.

6.4 Deposit characterization

For the deposit characterizations, piston deposits were collected from four specific locations after an "ISO load point" pre-ignition run through an engine disassembly. As a reference deposit, exhaust valve 2 oil deposits were collected through an optical access after an oil injector run ("ISO load point"). Figure

6-6 shows the specific deposit extraction points and the SEM secondary electron contrast images of the deposit samples.

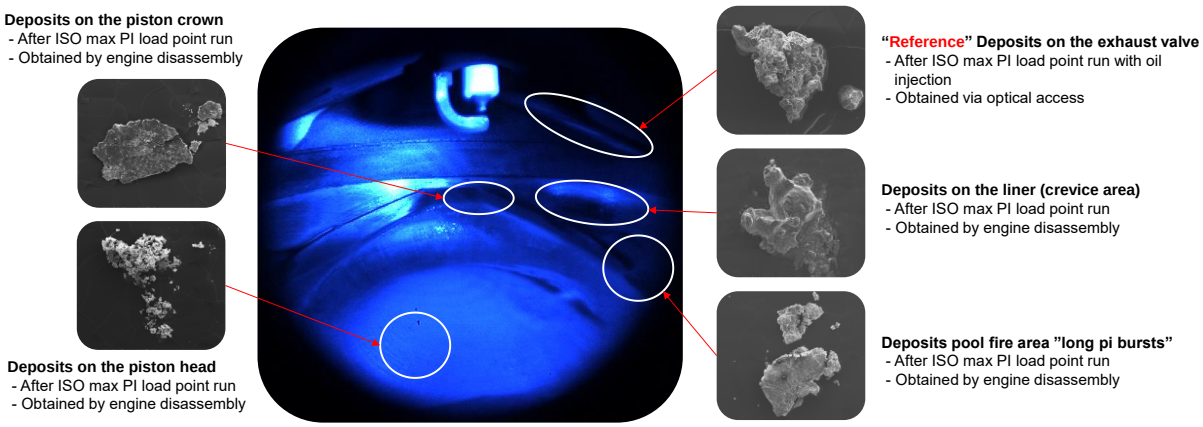

Figure 6-6: Combustion chamber deposit extraction areas.

SEM BSE and SEM EDX spectroscopy analysis

Figure 6-7 shows the SEM BSE and EDX spectroscopy analysis of the oil reference deposit. The EDX spectrum shows many oil (additive) element-specific peaks. The red spectrum corresponds to a contrast point analysis, the black spectrum to a grid averaging over the entire deposit sample. In addition to the main component carbon, many oil additive-specific elements can be seen. Among them is the element calcium, which has a strong influence on pre-ignition [22]. The Z-contrast image shows many high-contrast areas, which on the one hand indicates the general qualitative additive component distribution and, on the other hand, gives information about the element frequency. This allows a qualitative reference comparison with the analyses of the four "ISO load point" deposition samples.

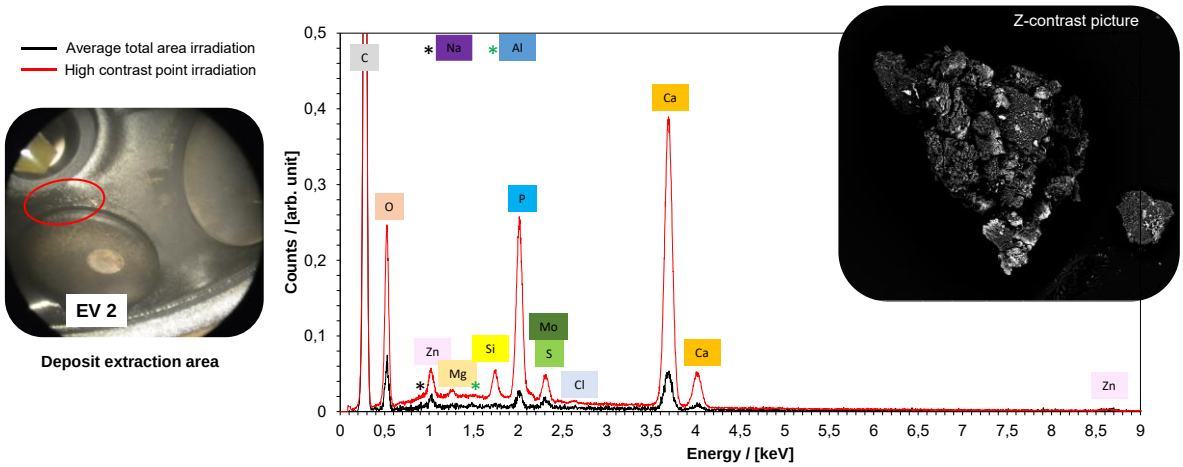

Figure 6-7: SEM BSE and EDX analysis of oil injection reference deposit.

Figure 6-8 shows the direct comparison of the SEM BSE and EDX spectroscopy analyses of the oil reference deposit to the deposits at the pool fire piston edge position (long pi series) and the deposits at the bore top/ crevice. The EDX spectra are very comparable. Thus, all deposits contain oil additive elements. The Z-contrast images show the most extensive accumulation of oil additive elements in the sample, which was involved in the initiation of the extremely long pi series. The bore top/ crevice sample,

on the other hand, shows only single contrast points. A correlation between oil additive components and pre-ignition potential can be assumed.

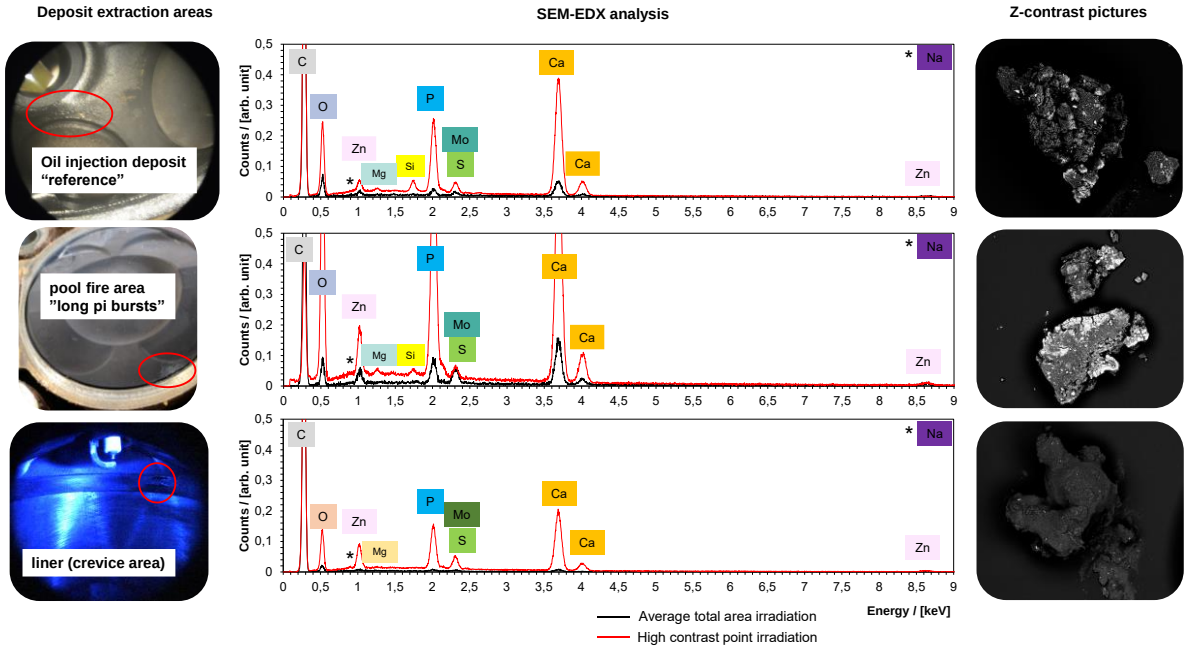

Figure 6-8: SEM BSE and EDX analysis of oil ash dominated deposits.

The deposits on the piston head and the piston crown show a completely different picture (Figure 6-9). Only in the deposit sample on the piston crown are traces of oil additive elements to be found. This could be an indication of the "physical enabling mechanism" of the fuel/ oil detachment from the piston crevice. In the deposit sample from the piston head, only elements of carbon and oxygen could be detected. The sample areas did not show any conspicuous behavior in the optical pre-ignition characterizations. Overall, there is a clear correlation between deposits with oil additive components and reactive combustion chamber locations. The EDX spectrum correspondence shows that the deposit caused by the spray/ liner interaction is also interspersed by the oil additive components. This also applies to the general deposits from the bore top/ piston crevice.

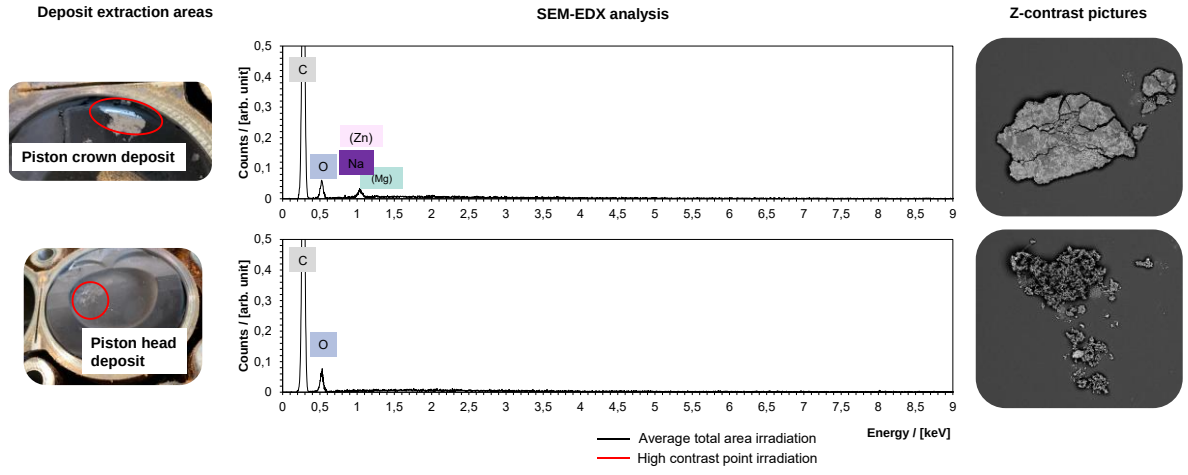

Figure 6-9: SEM BSE and EDX analysis of deposits with few oil ash components.

TGA oxidation reactivity analysis

With the help of thermal gravimetric analysis, the effect of the oil additive element inclusions in the deposits on their reaction potential can be investigated. Figure 6-10 shows the oxidative reactivity difference between deposit samples containing oil additive components and a deposit sample in which only carbon and oxygen could be detected. There is a clear difference in reactivity. Deposit samples that contain oil additive components show a significantly earlier oxidation behavior. A pure influence by the deposit morphology is excluded in the T_{MAX} range of 450°C [23]. It remains to be seen which exact effect this oxidation influence is based on.

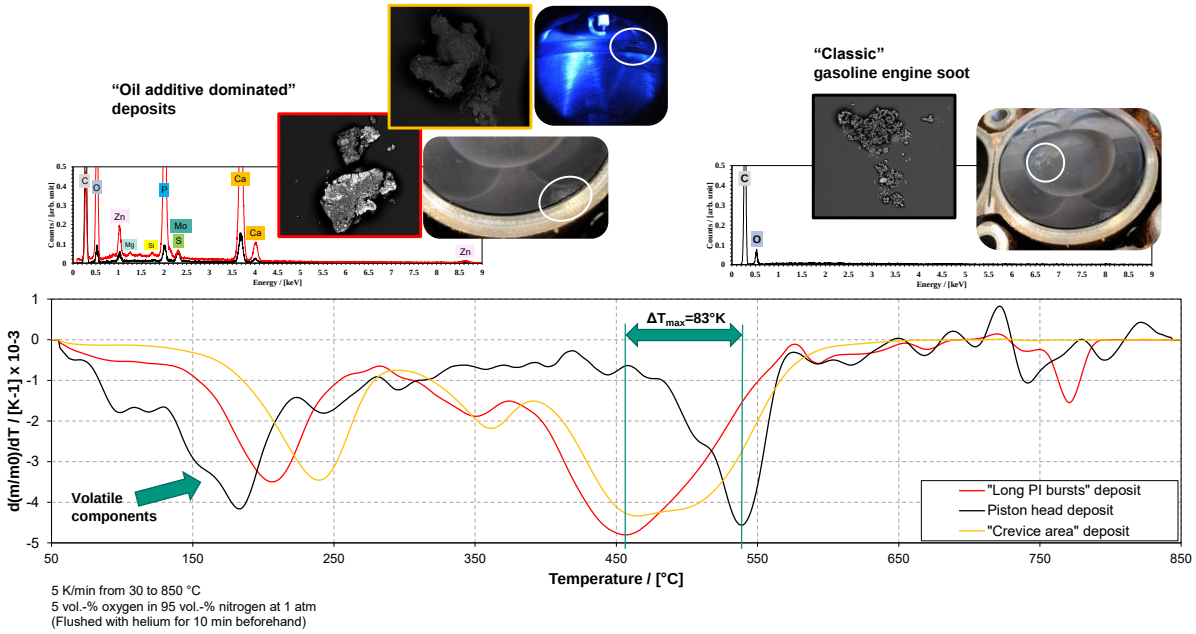

Figure 6-10: TGA comparison of deposits.

The reactive "deposit pattern" suspected in the oil injection tests can thus be confirmed. Specific combustion chamber deposits have oil additive components and thus have a greater reaction potential. This explains the occurrence of a constant deposit ignition source of extremely long PI series but also the formation of reactive particles and thus the general oil influence of the demonstrated pre-ignition mechanism.

7 Summary and conclusions

From the summary of all the knowledge and observations gained, the pre-ignition mechanism shown in Figure 7-1 is synthesized. There was no experimental and simulative evidence of oil droplet-induced pre-ignition. All optically detected pre-ignitions show a glowing surface deposition or particle history. The optical results and reactivity comparison of different specific deposits and their pre-ignition correlation shows that pre-ignition-initiating objects must be products of reactive deposits. The reactivity is increased by inorganic residues from oil additives.

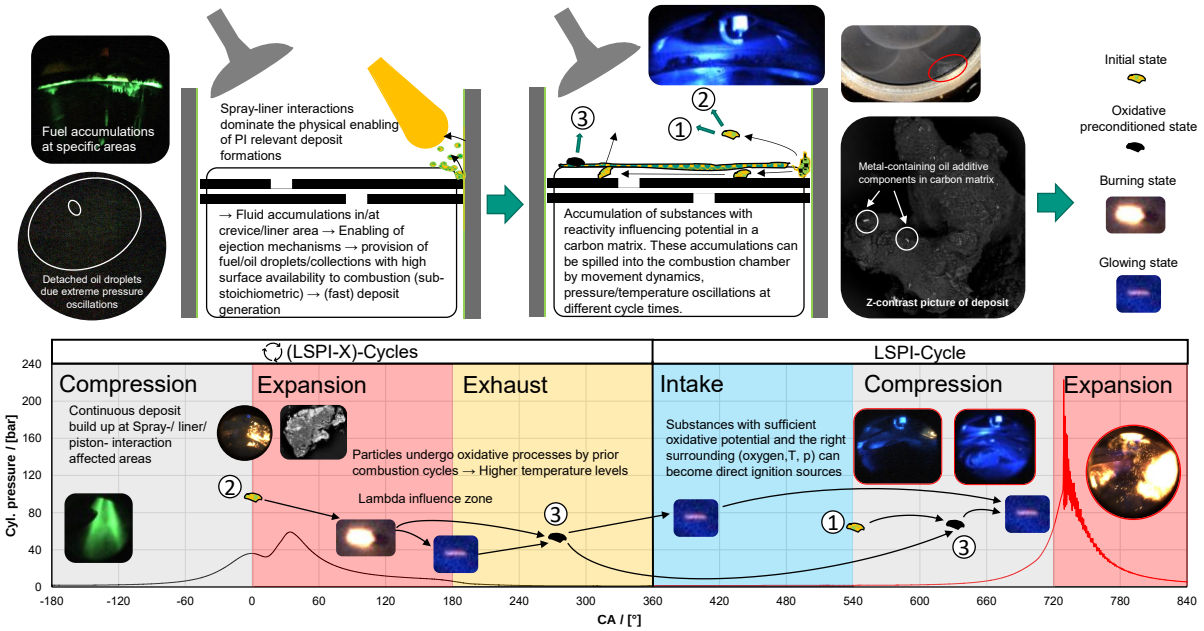

Figure 7-1: Derived pre-ignition mechanism.

The pre-ignition mechanism at hand is a complex multi-cyclic process. This initially consists of a "physical enabling mechanism." These are the initial processes that enable the subsequent formation of deposits of substances with reaction influence potential. Here, the spray/ liner interaction (oil film) is the dominant influencing factor. In particular, this enables under-stoichiometric oil combustion and thus creates the potential for reaction-influencing inorganic residues from oil additives to be deposited at piston crevice regions. Responsible for this can be the ejection of liquid or creep processes from the piston crevice due to an increased accumulation of oil and fuel and thus a change in surface tension and viscoelastic properties.

The subsequent iterative formation process of reactive deposits (deposit detachment by pre-ignition events) creates a further basis for the following pre-ignition initiations. For an efficient deposition of inorganic reaction-influencing substances from the oil additives, additional carbon deposition structures are necessary as carriers. These are formed by general sub-stoichiometric combustion of fuel and oil (pool fire areas). The fuel piston wetting point of the "ISO load point" at the piston top near the crevice area showed the highest density of reaction-influencing substances.

In the next step, these accumulations can be spilled into the combustion chamber by movement dynamics (piston ring, piston), pressure/ temperature oscillations at different cycle times. In the special case, with reactive deposits located on the piston crown and the associated oxygen availability as well as the possibility of a temperature increase through continuous exposure to combustion, local surface pre-

ignition initiations can occur (**3**). In the case that highly reactive particles are released, a sufficient temperature increase with simultaneous oxygen availability can lead to pre-ignition initiation (**1**). The extent to which thermal and oxidative preconditioning is necessary, which may enable this pathway in the first place, can only be conclusively clarified with complete knowledge of the deposit composition and the associated reactivity kinetics. Occurrences of series pre-ignition events could also correspond to this path.

A further initiation path (**2**) runs via the (necessary) participation of a reactive deposit particle in normal combustion cycles before pre-ignition. Hereby thermal and oxidative preconditioning can take place. This path thus shows a correlation between the air-fuel ratio and the probability of pre-ignition. It can also explain the often observed, intermittent subsequent pre-ignition behavior. We conclude a multicyclic "oil additive dominated" deposit-driven pre-ignition mechanism.

The outlined pre-ignition mechanism makes the stochastic nature of pre-ignition events comprehensible. The influence mechanisms of known "pre-ignition influencers" can also be explained. In the next step towards a complete understanding of the mechanism, the sub-mechanisms (physical enabling mechanisms, deposit building process, deposit chemistry) need to be precisely explored.

8 Appendix

8.1 Bibliography

1. Golloch R (2005), Downsizing bei Verbrennungsmotoren: Ein wirkungsvolles Konzept zur Kraftstoffverbrauchssenkung. VDI-Buch. Springer, Berlin.
2. Dahnz C, Han K-M, Spicher U et al. (2010), Investigations on Pre-Ignition in Highly Supercharged SI Engines. SAE Int J Engines 3:214–224.
3. Takeuchi K, Fujimoto K, Hirano S et al. (2012) Investigation of Engine Oil Effect on Abnormal Combustion in Turbocharged Direct Injection - Spark Ignition Engines. SAE Int J Fuels Lubr 5:1017–1024.
4. Luef R (2015) Entwicklung einer Prüfmethode zur Bestimmung des Öleinflusses auf irreguläre Verbrennungsphänomene bei hochaufgeladenen DI-Ottomotoren. Dissertation, Technische Universität Graz.
5. Zöbinger N, Lauer T (2020), Numerical Investigation of the Influence of Oil Dilution on the Ability to Initiate a Pre-Ignition Combustion," SAE Int. J. Advances & Curr. Prac. in Mobility 2(4):1935-1962, 2020, doi:10.4271/2020-01-0611.
6. Stauch, R., Lipp, S., Maas, U., Detailed numerical simulations of the auto-ignition of single n-heptane droplets in air. Combustion and Flame 2006:533–542.
7. J. C. G. Andrae, T. Brinck, G. T. Kalghatgi, (2008), HCCI experiments with toluene reference fuels modeled by a semidetailed chemical kinetic model. Combust. Flame 155: 696–712.
8. U. Maas J.Warnatz (1988), Ignition processes in hydrogen-oxygen mixtures. Combust. Flame 74, :53–69.
9. Aggarwal S,K., Single droplet ignition (2014), Theoretical analyses and experimental findings. Prog., Energy Combust. Sc 45 (2014)i: 79–107.
10. S. Fei, Z. Wang, Y. Qi, Y. Wang (2019,) Investigation on ignition of a single lubricating oil droplet in premixed combustible mixture at engine-relevant conditions. SAE Tech. Pap. 2019-01-0298.
11. Z. Wang, et al.(2016), Quantification of the Keto-Hydroperoxide (HOOCH2OCHO) and Other Elusive Inter-mediates during Low-Temperature Oxidation of Dimethyl Ether.

12. N. Blin-Simiand, F. Jorand, K. Keller, M. Fiderer, K. Sahetchian (1998) Ketohydroperoxides and ignition delay in internal combustion engines. Combust. Flame (112): 282–287.

13. Morgan, N., Smallbone, A., Bhave, A., Kraft, M., Cracknell, R., Kalghatgi, G. (ed) Mapping surrogate gasoline compositions into RON/MON space. Combustion and Flame 2010(157).

14. Kalghatgi, G. T., Bradley, D (2012) Pre-ignition and 'super-knock' in turbo-charged spark-ignition engines. International Journal of Engine Research 2012:399–414.

15. Livengood, J. C., Wu, P. C (ed), (1955) Correlation of Autoignition phenomena in internal combustion engines and rapid compression machines, Symposium on combustion, volume 5, 1955.

16. K. Nishikawi, N. Hafnan. (2000): The Determatoin of thermal properties of engine combustion chamber deposits . SAE technical paper, 2000-01-1215, 2000.

17. K. Li, Q. Liu, et al (2020): Investigation of the carbon structure of naturally graphitized coals from Central Hunan, China, by density-gradient centrifugation, X-ray diffraction, and high-resolution transmission electron microscopy. International Journal of Coal Geology 232,1036285.

18. Siemens (2017) Methodology STAR-CD Version 4.30.

19. X. Liang, Y. Wang and K. Wang et al., (2020) : "Experimental study of impact of lubricant-derived ash on oxidation reactivity of soot generated in diesel engines". Proceeding of the combustion institute 000, pp. 1-8.

20. S. Palaveev,(2018) "Untersuchungen zu den Ursachen von stochastischen Vorentflammungen bei aufgeladenen Ottomotoren," KIT, Diss. Forschungsberichte aus dem Institut für Kolbenmaschinen, ISBN: 978-3-8325-4705-9, 01/2018.

21. S. Pritze and A. Döhler, (2013), A contribution to better understanding the pre-ignition phenomenon in highly charged internal combustion engines with direct fuel injection. IAV, 4th Conference on Knocking in Gasoline Engines, Berlin 2013:41–61.

22. S. Hirano, M. Yamashita, K. Fujimoto and K. Kato, (2013), "Investigation of Engine Oil Effect on Abnormal Combustion in Turbocharged Direct Injection - Spark Ignition Engines (Part 2)," SAE International, doi:10.4271/2013-01-2569, 2013.

23. S. Koch, F. P. Hagen, H. Kubach, A. Velji and T. Koch, (2020) , "Impact of the Injection Strategy on Soot Reactivity and Particle Properties of a GDI Engine," SAE Technical Paper 2020-01-0392, 2020, doi:10.4271/2020-01-0392.